RL-TR-95-28
Final Technical Report
March 1995

DLMS-BASED OPTICAL MEMORIES

Hughes Research Laboratories

C.S. Wu, L.R. Dalton, and U. Efron

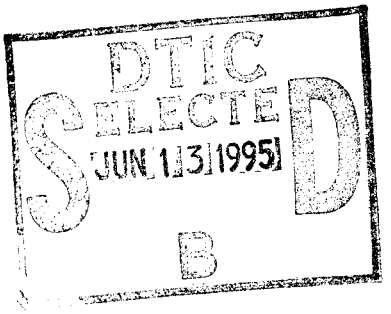

APPROVED FOR PUBLIC RELEASE; DISTRIBUTION UNLIMITED.

Rome Laboratory
Air Force Materiel Command
Griffiss Air Force Base, New York

This report has been reviewed by the Rome Laboratory Public Affairs Office (PA) and is releasable to the National Technical Information Service (NTIS). At NTIS it will be releasable to the general public, including foreign nations.

RL-TR-95-28 has been reviewed and is approved for publication.

APPROVED: Bernard J. Clarke

BERNARD J. CLARKE, Captain, USAF
Project Engineer

FOR THE COMMANDER: Anthony S. Szalkowski

ANTHONY S. SZALKOWSKI
Acting Technical Director
Intelligence & Reconnaissance Directorate

If your address has changed or if you wish to be removed from the Rome Laboratory mailing list, or if the addressee is no longer employed by your organization, please notify RL (IRAP) Griffiss AFB NY 13441. This will assist us in maintaining a current mailing list.

Do not return copies of this report unless contractual obligations or notices on a specific document require that it be returned.

REPORT DOCUMENTATION PAGE

Form Approved
OMB No. 0704-0188

1. AGENCY USE ONLY (Leave Blank)	2. REPORT DATE	3. REPORT TYPE AND DATES COVERED
	March 1995	Final Jun 93 - Oct 94

4. TITLE AND SUBTITLE

DLMS-BASED OPTICAL MEMORIES

5. FUNDING NUMBERS

C - F30602-93-C-0158
PE - 62702F
PR - 4594
TA - 15
WU - K6

6. AUTHOR(S)

C.S. Wu, L.R. Dalton, and U. Efron

7. PERFORMING ORGANIZATION NAME(S) AND ADDRESS(ES)

Hughes Research Laboratories
3011 Malibu Canyon Rd
Malibu CA 90265

8. PERFORMING ORGANIZATION REPORT NUMBER

N/A

9. SPONSORING/MONITORING AGENCY NAME(S) AND ADDRESS(ES)

Rome Laboratory (IRAP)
32 Hangar Rd
Griffiss AFB NY 13441-4114

10. SPONSORING/MONITORING AGENCY REPORT NUMBER

RL-TR-95-28

11. SUPPLEMENTARY NOTES

Rome Laboratory Project Engineer: Bernard J. Clarke, Captain, USAF/IRAP/ (315) 330-4581

12a. DISTRIBUTION/AVAILABILITY STATEMENT

Approved for public release; distribution unlimited.

12b. DISTRIBUTION CODE

13. ABSTRACT (Maximum 200 words)

The objective of this program is to prove the feasibility of room-temperature, erasable DLMS-based optical memories. To achieve the room-temperature spectral hole burning using the dye-labeled polymer microspheres, several materials issues (high-precision polymer microsphere distributions, photo-reversible photochromic dyes, and dye-microsphere coupling) have been addressed. Over 30 azobenzene dyes have been synthesized to meet the criteria for erasable persistent spectral hole-burning. Among them, aminosilfoneazobenzenes shows reasonable kinetics for photo-induced conformational changes. Technology advances in polymer-microspheres give us excellent control over average microsphere size, the dispersion of microsphere sizes in a preparation, and the properties of microsphere composites. Two chemical schemes have been developed to properly label the high-precision microsphere distribution with the bi-stable chromophores. During the program period, we successfully demonstrated the room-temperature Write/Erase/Read operations in the frequency domain. Multiple spectral holes were burned into the sample and successfully retrieved. The erasure of the stored spectral information was also achieved by a pure optical activation. Furthermore, we demonstrated the capability of rewriting new spectral information onto the erased sample.

14. SUBJECT TERMS	15. NUMBER OF PAGES
Optical memories, Persistent spectral hole burning, Spectral hole burning, Dye-labeled microspheres	52
	16. PRICE CODE

17. SECURITY CLASSIFICATION OF REPORT	18. SECURITY CLASSIFICATION OF THIS PAGE	19. SECURITY CLASSIFICATION OF ABSTRACT	20. LIMITATION OF ABSTRACT
UNCLASSIFIED	UNCLASSIFIED	UNCLASSIFIED	UL

CONTENTS

CONTENTS

ILLUSTRATIONS

Section 1
INTRODUCTION

Physical limitations such as spatial resolution, signal-to-noise ratio and cross talk, control the current performance of 2-D memories (both magnetic and optical). Present limitations are: (a) relatively low storage density ($\approx 10^8$ bits/cm^2), (b) low throughput rate ($\sim 10^6$ bits/sec) and (c) slow access time ($>10^{-3}$ sec). However, as information technology plays an increasingly important role in both military and commercial applications, more powerful computing power demands even larger data storage capacity than ever. Naturally, the data transfer rate and data access time of large-capacity data storage devices ought to be significantly improved so they will not become bottlenecks to the system[1]. For example, next generation supercomputers and real time data acquisition/processing and pattern recognition systems[2-4] will require higher storage density ($\times 10^4$), a higher throughput rate ($\times 10^3$) and faster access time ($\times 10^{-3}$). Yet despite intensive research efforts devoted to squeezing more capacity into the device, current 2-D optical storage technology may reach its theoretical limit of storage density, 10^8 bits/cm^2, by the end of this century[5]. In addition, parallel I/O and parallel processing, which can alleviate the throughput bottleneck, are rather difficult to implement in the current 2-D memory systems. Hence, to meet future needs for extremely high-density data storage devices, innovative memory principles are being eagerly explored.

The most natural approach to improve storage density is to extend the 2-D storage to multi-dimensional domains. Holographic data storage[6,7] and two-photon data storage[8] represent typical examples of packing data into a 3-D (X, Y and Z spatial dimensions) volume space. Another elegant approach relies on the introduction of the optical frequency as the additional storage dimension (wavelength multiplexing). Digital information may be encoded into the optical frequency domain and densely packed at the same spatial spot on the storage medium. While the Z dimension is usually limited by the optical depth of field, the large optical frequency dimension ($\sim 10^{14}$ Hz) can provide an extremely large multiplexing capability to significantly enhance data storage density.

The persistent spectral hole-burning (PSHB) effect in suitable materials was suggested to provide the frequency selectivity required for the wavelength multiplexing approach[9]. Resulting from strain-induced frequency shifts on the atomic or molecular resonance, homogeneous absorption lines of optically active centers are inhomogeneously broadened[10]. Each individual homogeneous line within the inhomogeneously broadened band may be selectively excited by a narrow-band optical excitation, on the condition that the excitation frequency is in resonance with the transition frequency of the particular homogeneous line. As most of the molecules relax back to

the initial state, a small fraction of the excited molecules may undergo a photochemical or photophysical transformation and relax to a different ground state. This photoreaction generally produces photoproducts with a modified absorption spectrum[1]. Since those photoproducts will not contribute to the absorption at the particular excitation wavelength, this will result in a dip (spectral hole) in the inhomogeneously broadened absorption band. The bandwidth of the spectral hole is on the order of twice the corresponding homogeneous linewidth[11]. This phenomenon provides a fundamental ground for encoding and retrieving multiple digital information in the frequency domain.

The number of spectral holes which may be independently excited depends on the ratio of the inhomogeneous to homogeneous linewidth, the frequency multiplexing factor. At the same time, the homogeneous linewidth of a given material system strongly depends on the operation temperature. In principle, the frequency multiplexing factor can be as large as 10^6 if ultralow cryogenic temperature is permissible[12]. Since thermal energy can activate the transition and significantly broaden the homogeneous linewidth[10], it is generally necessary to maintain the operation in a cryogenic environment. An estimation has indicated that the frequency multiplexing factor may reach ~400 at 77K and that it will quickly drop to ~20 at room temperature[13]. Although low temperature (~4K) may be reliably accomplished using commercially available cryocoolers, this requirement may prove to be too stringent for the commercial market. For practical high-density storage applications, it has even been suggested to pursue higher operation temperatures (for example, room temperature) at the expense of lower multiplexing factors[14].

The recognition of the need for high temperature spectral hole-burning has stimulated increasing research efforts in material development and physical configurations. For example, intensive studies have been devoted to development of room-temperature PSHB materials such as organic solutions[15], Sm^{2+}-doped crystals[16-18], and Sm^{2+}-doped glasses[13,19-21]. In this research, two to three spectral holes were successfully burned into the samples and retrieved at room temperature. In addition, a new room-temperature PSHB mechanism has been proposed and observed in dye-labeled microparticles[22]. Spectral hole-burning was also recently observed in sol-gel CdS quantum dots at room temperature[23].

For this program we proposed to develop a high dimensional 3-D/4-D Write/Erase/Read (W/E/R) optical memory system with parallel access capability allowing a fast data transfer rate. Current research effort is aimed at developing an erasable wavelength-multiplexing scheme operating at room temperature. The Dye Labeled Micro Sphere (DLMS) erasable memory utilizes inherent Morphology Dependent Resonances (MDRs) of microspheres for the necessary wavelength selectivity. The sharp MDR homogeneous lines characterize the interaction of light with a high precision microsphere at ambient temperature[24]. An inhomogeneous distribution of multiple narrow resonance lines, representing slight changes in the microsphere sizes, will result in

a broad overlapped spectrum composed of the separate but slightly shifted resonances. As each individual resonance is defined mostly by the quality factor (Q-value) of the corresponding microsphere morphology, this arrangement will result in sharp homogeneous resonance lines inhomogeneously broadened at ambient temperature[22]. These sharp resonances will correspond to frequency slots in the spectrum that can be individually encoded by the writing light.

The data encoding is based on the direct interaction of writing photons with the electrons in bi-stable dye molecules to induce a reversible photochromic isomerization process. As the dye molecules are transformed to the encoded isomeric phase, they will be distinguished by a change in their chemical configuration resulting in a different spectral signature. Attaching these molecules to the surfaces of a high precision microsphere distribution allows the isomerization which occurs resonantly in only one particular microsphere morphology (within a specified spectral range). The writing process will eliminate the particular homogeneous resonance line from the inhomogeneous distribution. As illustrated in Figure 1-1, multiple images may be encoded and stored in the optical frequency domain. The use of a relatively broad spectrum of the bi-stable dye permits us to "burn" multiple narrow-band spectral holes in the system, thus achieving a large magnitude wavelength multiplexing factor for high-density data storage. Furthermore, the introduction of the bi-stable dyes also opens the door to satisfying the need for erasable memory systems.

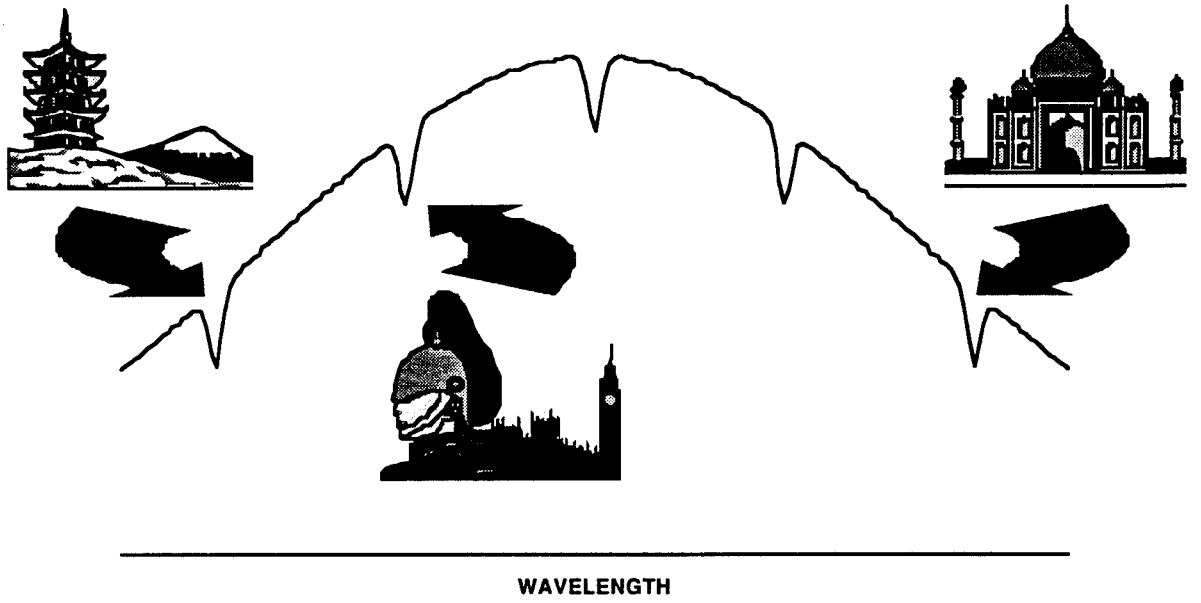

Figure 1-1. Multiple spectral holes can be burned into the sample to store many 2-D images.

A conceptual schematic of the DLMS 3-D/4-D optical storage system is depicted in Figure 1-2. The 3-D/4-D memory system is designed to provide parallel addressing, Write, Read and Erase operations. Writing will be accomplished by tuning a high power tunable laser to encode the

frequency data onto the N×N pixel matrix, modulated by a high resolution Spatial Light Modulator (SLM). The data will be encoded by shifting absorption frequencies of the dye-labeled microspheres out of the spectral range of interest. The "burned" frequency holes will be retrieved in parallel by scanning with a low power tunable laser in the MDR range and monitoring the absorption or the fluorescence in each pixel as a function of the frequency.

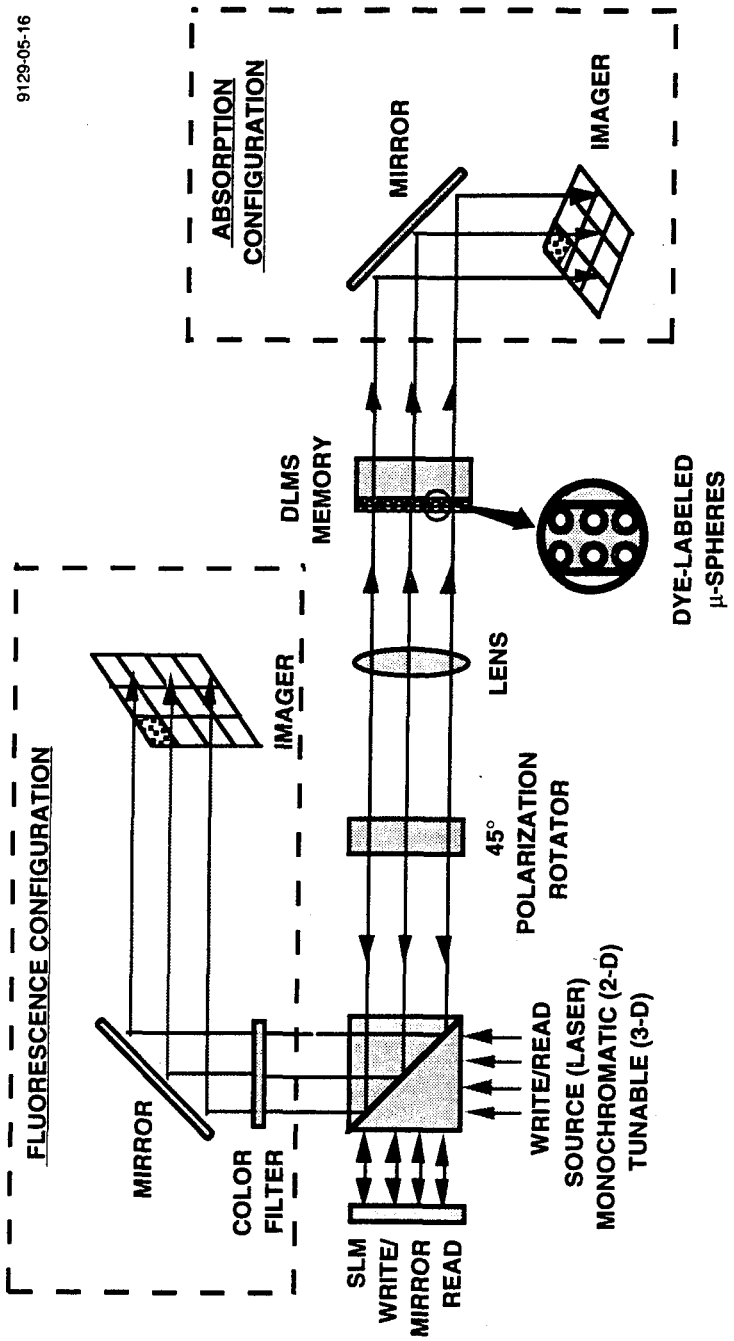

Figure 1-2. 3-D/4-D dye-labeled micro-spheres (DLMS) optical memory system.

To achieve room-temperature spectral hole-burning using dye-labeled polymer microspheres, the following materials issues must be and have been addressed in research: (1) polymer microspheres of dimensions ranging from several hundred nanometers to 20 μm must be synthesized with good control of the distribution of microsphere sizes and the chemical contamination of the sphere surfaces; (2) appropriate photochromic dyes must be developed which permit the desired optical changes to be effected, read or detected, and erased; and (3) dyes must be attached to microspheres in a controlled manner so that the appropriate index of refraction coating is greater on the microsphere surface. During this program period the main research goal, a feasibility demonstration of DLMS-based erasable memory operations, has been successfully completed. The accomplishments of all technical tasks are summarized as follows.

1.1 SYNTHESIS OF PHOTOCHROMIC CHROMOPHORES

The efforts include the synthesis and evaluation of several bi-stable photochromic dye systems and selecting the best candidates for the DLMS-based data storage feasibility study.

1.2 SYNTHESIS OF POLYMER MICROSPHERES

A high precision DLMS distribution is essential to the 3-D/4-D optical memory system. The control of intermolecular interactions is extremely important in avoiding aggregation effects, which will degrade the Q-values of the MDR's. Techniques have been developed that permit preparation of linear microsphere-size gradient distributions.

1.3 CHROMOPHORE-MICROSPHERE COUPLING

Work has also progressed on coating microspheres with bi-stable dyes. Two different dye coupling methods have been developed to properly label the high-precision microsphere distribution with the bi-stable dye candidates.

1.4 FEASIBILITY DEMONSTRATION OF AN ERASABLE DLMS MEMORY SYSTEM

On the basis of all the above development tasks we have reduced the DLMS concept to practice and successfully demonstrated the room temperature W/E/R operations in the frequency domain. Multiple spectral holes were burned into a sample and successfully retrieved by scanning the wavelength of the laser probe beam. The erasure of the stored spectral information was achieved by a pure optical activation (through UV exposure). Furthermore, we also successfully demonstrated the capability of rewriting new spectral information onto the erased sample. During the research period we also improved the spectral hole-burning process in a non-erasable DLMS-based memory system. Nine spectral holes were frequency-encoded and retrieved within a spectral

range of 20 nm. To our best knowledge this is the largest multiplexing factor that has been reported in the room temperature spectral hole-burning process.

1.5 ORGANIZATION OF THIS REPORT

The remainder of this report consists of five parts: First, we review the DLMS technical concept in Section 2. In Section 3 the search for suitable bi-stable dyes, essential for the erasable DLMS-based memory operations, is discussed. Next, in Section 4, the fabrication of high-precision polymer microspheres, critical to the room temperature MDR-based wavelength multiplexing approach, is described. The detailed chromophore/microsphere coupling technique is discussed in Section 5. Finally, the experimental verification of the room-temperature, erasable DLMS-based memory operations is presented in Section 6. In addition, our study of the multiple spectral hole-burning process in non-erasable DLMS-based memory system is attached in Appendix.

Section 2
DLMS TECHNICAL CONCEPT

2.1 GENERAL

The program for developing the DLMS-based memory technology is aimed at achieving high density (wavelength multiplexing), high throughput, and erasable optical memories operating at ambient temperature. Wavelength multiplexing is based on the PSHB concept, which uses the spectral information to identify the data sequence. The idea was first introduced by Castro, et al. for long-term data storage[9] and since then it has attracted worldwide research interest for its potential application in high-density data storages[14,25,26]. The inhomogeneous distribution of multiple narrow-band homogeneous resonances results in a smooth broad spectrum composed of a superposition of the slightly shifted resonances. The elimination of a particular homogeneous resonance from the smooth spectral distribution by the photo-isomerization process, will result in the formation of a "persistent hole" in the spectrum that can be detected (read out) as the encoded information. The requirement of spectrally sharp homogeneous resonances would normally dictate low operating temperatures. This condition is impractical in many data storage systems, especially for military applications[10]. In this program we use a microsphere distribution of controlled size, which is characterized by the narrow electromagnetic Morphology Dependent Resonances (MDRs) at ambient temperature, to replicate the inhomogeneously broadened homogeneous lines. This arrangement allows us to densely encode digital data in the optical frequency domain at ambient temperature.

Data storage is based on the direct interaction of writing photons with the electrons in bi-stable dye molecules, which will induce a reversible photo-isomerization. The bi-stable isomers are distinguished from each other by their spectral signatures allowing the utilization of different wavelengths for the memory operations. The isomeric bi-stable photo-chemical transformation will allow the utilization of photons for W/E/R operations in a high density optical memory. Because these photo-chemical transitions are involved only with the redistribution of local electron energy levels in the dye molecules, the transitions can be very fast and readily multicycled without the aging problem.

2.2 MICROSPHERE DISTRIBUTION AND MDR

It has been well-studied and understood, both theoretically and experimentally, that microspheres can act as high Q-value optical cavities with feedback provided by a total internal reflection at the interface (with a discontinuity in the index of refraction). A high Q-value optical cavity is provided whenever the size parameter ($2 \pi a / \lambda$, where a is the microsphere radius and

λ is the vacuum wavelength) satisfies the resonance conditions[24]. The resonances occur as a result of phase matching after the optical wave propagates successive trips around the circumference of the microspheres and returns to the starting point. The sharp MDR's associated with the microspheres provide the fundamental wavelength multiplexing tool allowing room temperature operation.

The Mie theory predicts that the MDR's will occur at optical wavelengths proportional to the sizes of the microspheres[24]. Here we can take advantage of these narrow-band MDR lines from the microspheres with their average radii close to the optical wavelength, to encode information in the frequency domain. Using well-established chemical techniques, polystyrene microspheres can be fabricated and columnar separated with 0.1 nm dimensional tolerances. The MDR's of these high precision microspheres are expected, according to the Mie theory, to exhibit high Q-values. The microspheres can then be labeled with a bi-stable dye. Each of the dye's two configurations is stable but photo-reversible at ambient temperature. The data will be encoded through the broad spectral absorption lines of the isomeric dyes to result in an erasable 3-D memory system (X, Y, ω). A similar concept was recently demonstrated for a read-only-memory (ROM) recording by Arnold et al[22,27]. The development of the photochemical reversible dyes and their attachment to the microspheres for an erasable memory system are the main improvements over the initial concept which they introduced.

2.3 W/E/R OPERATIONS IN THE FREQUENCY DOMAIN

According to the Mie theory, the optical susceptibility of the microsphere surfaces and the surrounding medium will determine the boundary conditions of Maxwell's equations and therefore determine the condition for the MDRs. When the size parameter of a particular dye-labeled microsphere matches natural resonant conditions, the internal field within the microsphere is expected to be relatively large[24]. Enhancements of absorption at the excitation wavelength, associated with the resonance for the given size of microspheres, can be anticipated. The writing light will transform the dye molecules to the encoded isomeric phase, which is distinguished by a different spectral signature. The enhanced interaction of the writing monochromatic photons with the sharp resonances will preferentially promote the photo-isomerization which occurs in a selected microsphere distribution. This will result in the removal of the spectral "slot" of the photo-addressed microspheres from the broad spectral band of the dye/microsphere distribution, thus encoding the appropriate frequency slot in the broad inhomogeneous spectrum (in accord with the PSHB process). The sharpness of the resonance cavities will depend on the Q-values of their morphological structures and the boundary conditions. Since a broad absorption spectrum is provided by the bi-stable dye, a large wavelength multiplexing factor can be achieved in the DLMS-based memory system.

The readout of the encoded PSHB information can be achieved by scanning the frequency of a low intensity narrow-band light source and *in-situ* monitoring either the light absorption or the characteristic fluorescence. The encoded frequency slot will be detected by the absence of the resonant MDR absorption or the characteristic fluorescence. The signal-to-noise ratio (S/N) of the readout depends on the contribution of the encoded resonance at the frequency slot versus the total contribution of the non-encoded microspheres. Increasing the Q-values of the MDR, by controlling precisely the microsphere dimensions and the boundary conditions of the optical susceptibilities, will allow highly defined frequency slots to be "burned" with a low intensity tunable laser. In the meantime the high Q-values will also allow the utilization of extremely low-level scanning light for detecting the encoded PSHB, without activating the un-encoded frequency slots.

The memory erasure may be carried out using the appropriate wavelength light source. This wavelength must be different from that used for the hole-burning. The process will transform the bi-stable dye back into its original phase. Again, the photoreactions mainly redistribute the local electron energy levels in the dye molecules, so that the erasure process may be multicycled without causing a serious aging problem.

Section 3
SYNTHESIS OF PHOTOCHROMIC CHROMOPHORES

3.1 GENERAL REQUIREMENTS

In general dye molecules must satisfy a number of properties for use in optical memory applications based upon persistent spectral hole-burning:

- They must exhibit large (e.g., OD changes from greater than 2.0 to less than 0.2) changes in optical absorption associated with light-induced changes in molecular conformation. For example, a large change may be associated with a change in π-electron delocalization which in turn depends upon orbital overlap (molecular conformation).
- The search for the dye suitable for room temperature wavelength multiplexing must accompany with high efficiency for spectral hole formation. In addition, a fast isomerization rate should be accompanied with the photochromic dyes to ensure a high data transfer rate desired for large storage-capacity memories Thus, laser-induced conformational changes should be fast for modest laser powers (e.g., 0.5 to 20 mW/cm^2). Again, π-electron materials are attractive because of large oscillator strengths.
- Laser-induced conformational changes should be stable for long periods of time (e.g., days to years) so that memory is long term and is changed only by the laser-induced erase operation. This time is determined by steric hindrance in the spatial region of the conformational change.
- Reversible laser-induced cycling between two molecular conformations is required. Both states must be stable and no electron transfer occurs during the process. It is crucial to avoid side reactions.
- Ideally, the photochromic dye should exhibit a strong fluorescence to yield better signal-to-noise in the read operation.
- If 4-D memory is desired, the chromophore is preferred to exhibit a two photon absorption.
- The dye must be functionalized to permit attachment to the polymer micro spheres.
- Examples of laser-induced processes which may be appropriate for exploitation include photo-induced
  - trans-to-cis isomerization as found in azobenzenes, stilbenes, etc.
  - ring opening reactions as found in spiropyrans, etc.
  - keto-enol tautomerism (photoenolization)
  - interconversion between twisted intramolecular charge transfer (TICT) states
  - conversion of nitrones to oxaziridines

- interconversion between liquid crystalline states
- photodegration (chemical interconversion) which is typically an irreversible process however it is conceivable that some example might be found where the material could be regenerated.

Although considerable work was carried out with the chromophore Nile Red, the photochromic process for this material is irreversible photochemical decomposition which can be used only to produce read-only memories. Since the principles involved in employing this dye are identical to those of azobenzenes (which we will discuss at length), we will not explicitly discuss the materials synthesis issues for Nile Red materials.

3.2 PHOTOREVERSIBLE CHROMOPHORES: AZOBENZENES

Azobenenes have attracted considerable attention for the fabrication of write-read-erase memories. With the exception of the requirement of a two-photon process they satisfy to some extent all of the above criteria. The most significant weakness is low fluorescence quantum efficiency for most members of this series. To overcome this limitation, we synthesized approximately 30 new azobenzene dyes and evaluated their fluorescence. Most did not meet our criteria and were examined no further. However, moderately strong fluorescence together with reasonable kinetics for photo-induced conformational changes were observed for aminosulfoneazobenzenenes such as shown below (Figure 2-1)[28,29].

This synthesis scheme illustrates the critical features of preparing chromophores; namely, (1) the fundamental reaction scheme for preparing azobenzenes from commercially available starting materials, (2) the procedure used to modify optical properties by derivatization, and (3) the procedure for addition functionalities to permit covalent coupling of the chromophores to polymer structures and to other chromophores (a key feature of this latter activity is the development of a double-end crosslinkable (DEC) chromophore—a methodology pioneered at USC in the past three years. The synthesis scheme shown in modified in straightforward ways to incorporate different donor and acceptor groups to modify optical properties and to incorporate different coupling functionalities to modify the covalent coupling between chromophore and polymer and between chromophores. The example shown was also shown because it illustrates the introduction of both addition and condensation coupling functionalities. These are the fundamental chemical processes that we exploit in synthesizing polymer microspheres with covalently coupled dye layers.

3.3 DISCUSSIONS

Note that index variations between the polymer core and the chromophore surface layer will clearly influence morphological resonances (e.g., the quality factor Q-values). This variation can be influenced either by attempting to systematically vary the structure of the chromophore, by varying the chromophore number density in the surface shell, or by varying the thickness of the

shell. It work carried out to date we have focused upon control achieved by varying the thickness of the chromophore coating layer.

Some flexibility in terminating the chromophore is also desirable from the standpoint that we have shown the speed of the writing operation is dependent upon the exact structure of the chromophore. This includes exactly the nature of the coupling at both ends of the chromophore.

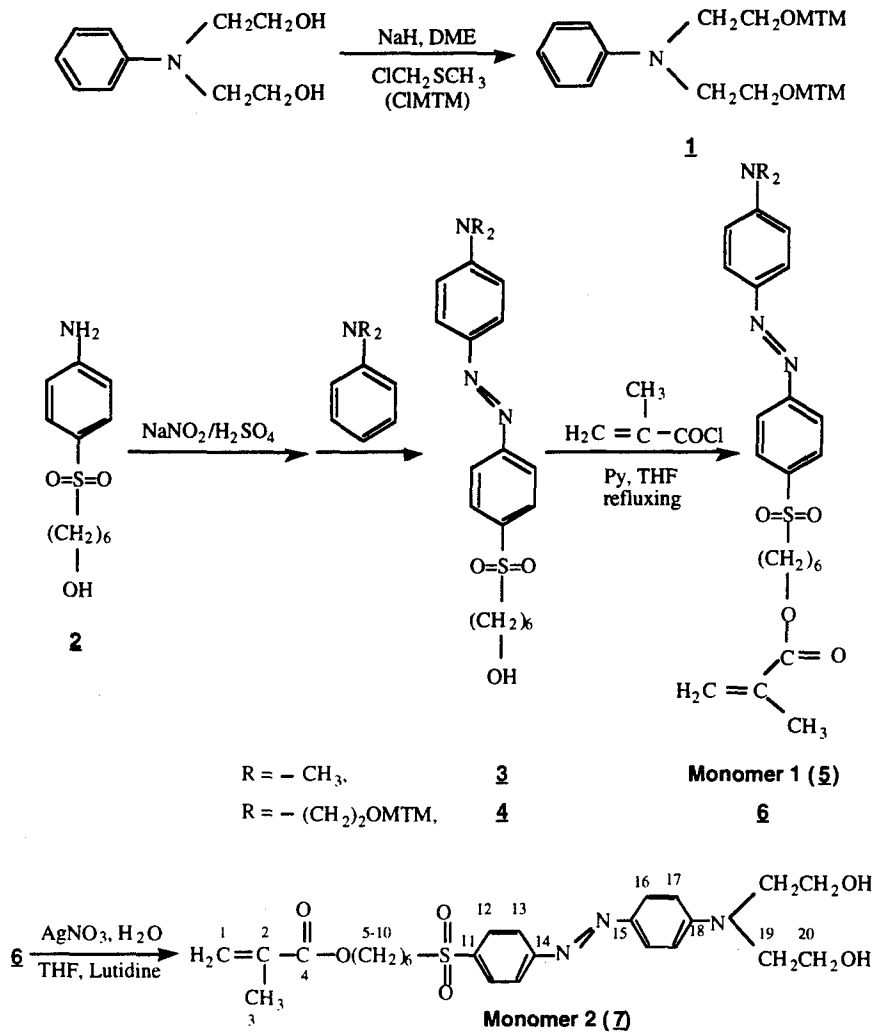

Figure 2-1. Reaction scheme for the syntheses of Amino-sulfone azobenzene chromophores.

Section 4
SYNTHESIS OF POLYMER MICROSPHERES

4.1 GENERAL RESEARCH ACTIVITIES

The DLMS memory system requires polymer microspheres of a size comparable to the optical wavelength or a multiple thereof. The following crucial activities have been addressed in the synthesis of microspheres.

- Since a broad size distribution would lead to poor signal-to-noise in spectral hole-burning, a uniform size of microspheres is desired. Techniques have been developed for preparing crosslinked spherical polymer beads monodisperse in size [J. Polym. Sci., 28, 1909, 2707 (1990)]
- The wavelength selectivity strongly depends on the Q-values of the MDRs associated with the microspheres; The polymer microsphere surface should be smooth and free of contaminating impurities, surface impurities may both degrade the Q-values of the MDRs and may interfere with functionalization of the surface. Polymerization is conducted in aqueous emulsion in the absence of emulsifier, so that bead surfaces are uncontaminated.
- Bead compositions include polystyrene, polymethyl methacrylate, polyethyl methacrylate, polybutyl methacrylate and polymethacrylonitrile
- Crosslinking was accomplished by copolymerizing styrene with divinylbenzene and methacrylates with ethylene glycol dimethacrylate
- Syntheses have been scaled up to a volume of 3 liters and microsphere yields up to 200 grams per run have been achieved
- Monodisperse microsphere diameters are controlled between 150 and 800 nm in a single stage synthesis and crosslink densities are varied up to 20 mol %
- Extensive kinetic studies establish a monotonic growth of spherical beads with conversion, as the number of microspheres appears to be fixed very early in the reaction
- With repeated seeding using preformed microspheres, compositionally complex spherical beads up to 4 mm in diameter were obtained, consisting of core and shells of controlled composition
- Polystyrene beads up to 20-μm diameter have been prepared by seeded polymerization.

4.2 SYNTHESIS OF POLYMER MICROSPHERES

We have exploited the capabilities developed by our former colleague, Professor John Aklonis, and our current colleague, Professor Ronald Salovey, in preparing polymer micro spheres by emulsion polymerization without surfactant[30-40]. We have investigated polymerization of the

following monomers: styrene. p-acetoxystyrene, alkyl methacrylates, and methacrylonitrile. We have also investigated polymerization reactions in the presence of crosslinkers and water soluble initiators. Several factors are particularly important for producing micro spheres of high quality. These include maintenance of a constant ratio of monomer and crosslinker and control of temperature and shear rates during stirring. For example, in the emulsion polymerization of styrene, optimum results were obtained if the 1,4-divinylbenzene to styrene ratio was kept constant by using a semi-continuous process. In batch reactions, sphere size can be varied between 150 and 1000 nm with size distributions controlled to less than one percent. Syntheses have been scaled up to produce up to 200 grams of material. Kinetic studies show that the number of spheres is established early in the reaction and that the size of the micro spheres increases with time in a predictable manner.

Once the concentration of reactants has been selected, bead sizes are primarily determined by polymerization temperature and conversion. Therefore, the greater the temperature uniformity, the narrower the size distribution. Moreover, isolating beads at controlled conversion allows more precise definition and sharper distributions. To further maximize bead size uniformity, we developed a continuous process for bead synthesis. Appropriate design of monomer and initiator feed streams allowed precise control of crosslink density and compositional gradients. Continuous removal of the bead latex at specified rate yielded highly uniform particles. Electron micrographs of polymer microspheres are shown in Figure 4-1.

The crosslink density of the microspheres, controlled by the fraction of crosslinking monomer (Note: In one of our approaches this monomer also contains the photochromic dye), can be varied between 1 and 20 mol percent. Crosslink densities were determined using a newly developed procedure involving equilibrium swelling on an ultrafiltration membrane. With repeated "seeding" using preformed beads, compositional complex (e.g., dye labeled) spheres could be obtained, as large as 4 μm (Note: actually surface labeled beads can be obtained to 20 μm size) with core and shells corresponding to different polymers.

Previous research has led to several techniques for mixing micro spheres with a host matrix. These include: (a) high shear mixing in the presence of antioxidant, (b) the suspension of spheres in solutions of the polymer matrix followed by precipitation, and (c) the coagulation of polymer lattices consisting of emulsions of both crosslinked and uncrosslinked polymer particles.

Melt rheology studies of the resulting compatible and incompatible polymer micro sphere-polymer matrix composites, focused on several systems including polystyrene (PS) and polymethyl methacrylate (PMMA) beads in PS and PMMA matrices. Pronounced non-Newtonian behavior indicating considerable clustering is observed in the case of incompatible polymers, especially at low shear rates. An important finding is that the nature of the bead surface determines the degree of micro sphere clustering.

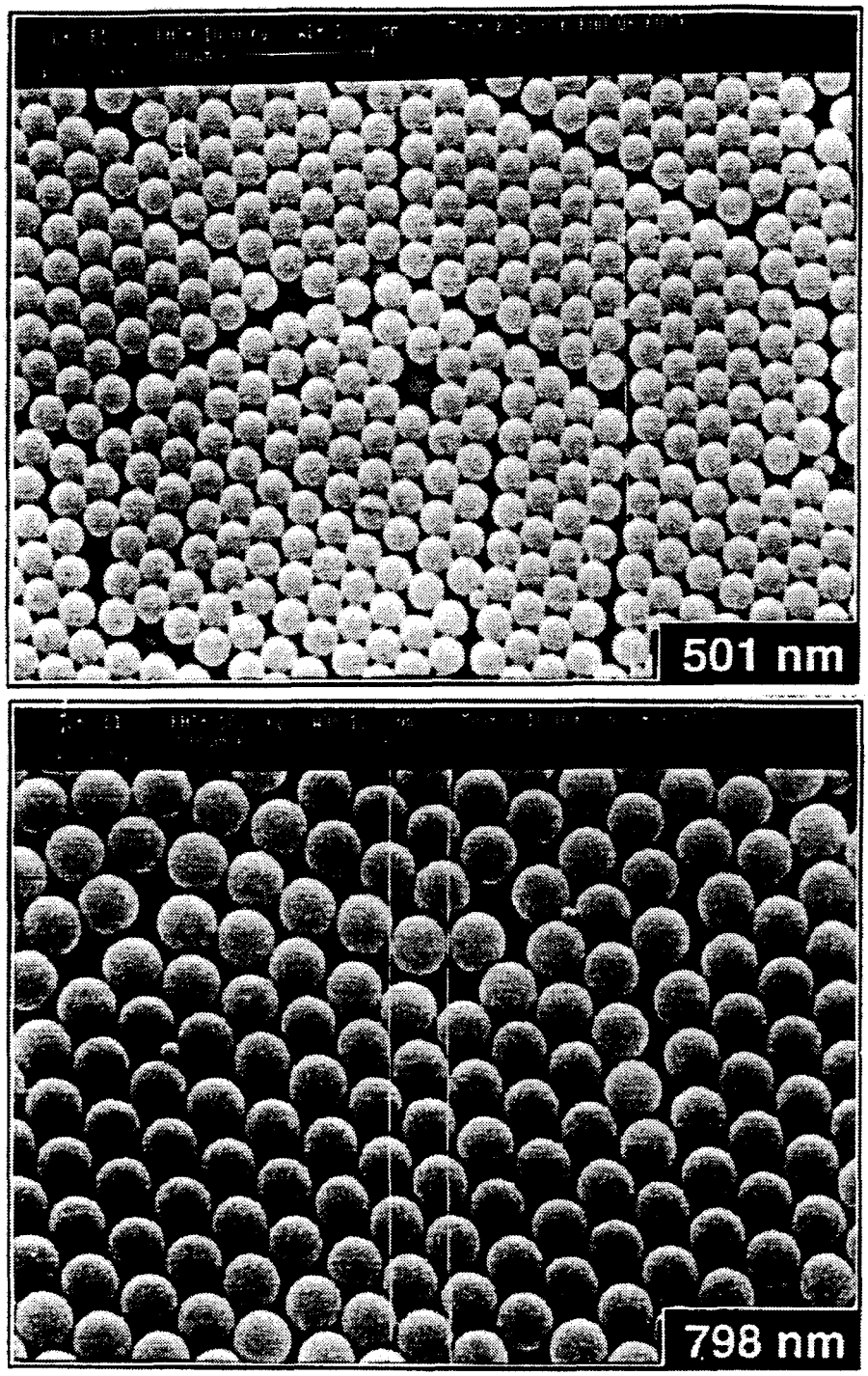

Figure 4-1. (a) Micrographs of various polystyrene microsphere size distributions.

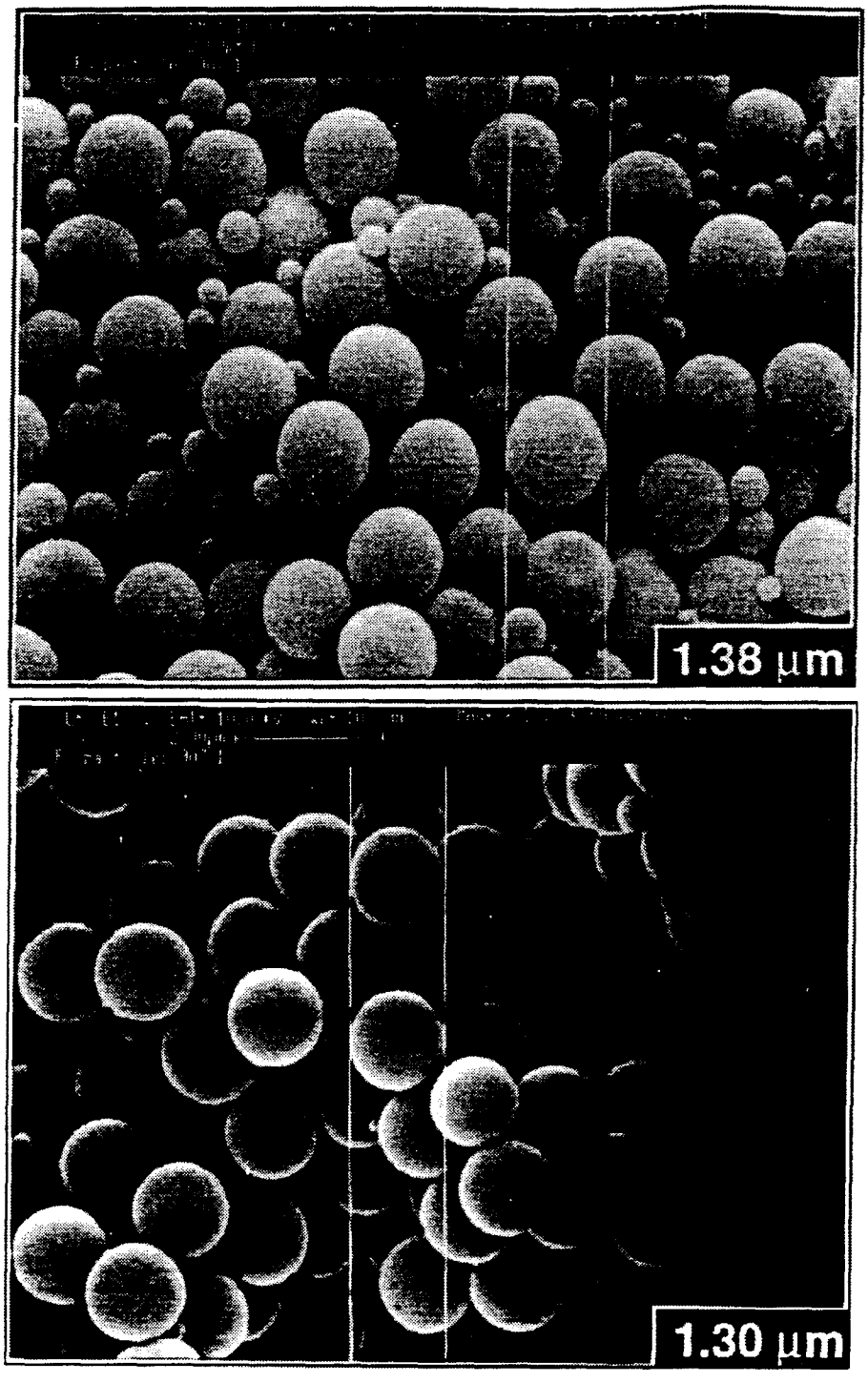

Figure 4-1. (b) Micrographs of various polystyrene microsphere size distributions.

4.3 DISCUSSIONS

In summary, the preparation of polymer micro spheres is a technology that is reasonably well in hand. Excellent control can be realized over average bead size, the dispersion of bead sizes in a preparation, over the spatial composition in compositionally complex (more than one type of polymer appearing in various shells) beads, and over the properties of bead composites.

Section 5
CHROMOPHORE-MICROSPHERE COUPLING

5.1 CHROMOPHORE-MICROSPHERE COUPLING METHODS

A central materials issue in exploitation of morphological resonances is the coupling of chromophores to polymer microspheres. We have developed two rather different schemes for coupling write-read-erase chromophores (WRECs) to polystyrene microspheres (PSMSs). The first is to synthesize a chromophore terminated by a vinylbenzene (styrene) functionality. Such a chromophore can be used as a comonomer with styrene and divinylbenzene in the polymerization reaction to form PSMSs. A chromophore coating of controlled variable thickness is produced by altering the monomer feed during the controlled growth of PSMSs. Up to a given point the feed is vinylbenzene and divinylbenzene which is then switched for an appropriate period of time under controlled reaction conditions to vinylbenzene-chromophore and divinylbenzene feed. The procedure for synthesis of such chromophores is analogous to that shown in the preceding section as one desires an addition functionality on one end and a condensation functionality on the other end. Multiple chromophore layers can be fabricated by condensation reactions between hydroxyl terminated chromophores using isocyanate coupling reagents.

The second approach is to derivatize the surface of PSMSs to permit covalent coupling of functionalized dyes. Their are two convenient schemes for functionalizing PSMS surfaces; the first yields a hydroxyl functionality[41] while the second yields-an amine functionality[42]. Hydroxyl groups can subsequently be reacted with acylchlorides, isocynates, acetic anhydrides, silyl halides, etc. to provide a coupling between chromophore and the PSMS surface. Many of the same condensation reactions apply to amines. Functionalization of the other end of the chromophore permits subsequent layers of dyes to be incorporated. Several schemes for hydroxylation and amination have been demonstrated. Two representative approaches are given below:

Hydroxylation

$$(\text{PSMS}) + \text{NaBO}_3(4\text{H}_2\text{O}) \longrightarrow (\text{PSMS})\text{-}(\text{OH})_x \qquad (5\text{-}1)$$

$$Me_3SiN_3 + 2F_3CSO_3H \longrightarrow NH_2N_2^+ - OSO_2CF_3 + Me_3SiOSO_2CF_3 \qquad (5\text{-}2)$$

$$(PSMS) + NH_2N_2^+ - OSO_2CF_3 \longrightarrow (PSMS) - (NH_2)_x \qquad (5\text{-}3)$$

Once hydroxyiated beads are obtained, dyes can be coupled by condensation reactions such as the acyl chloride-hydroxyl reaction shown below.

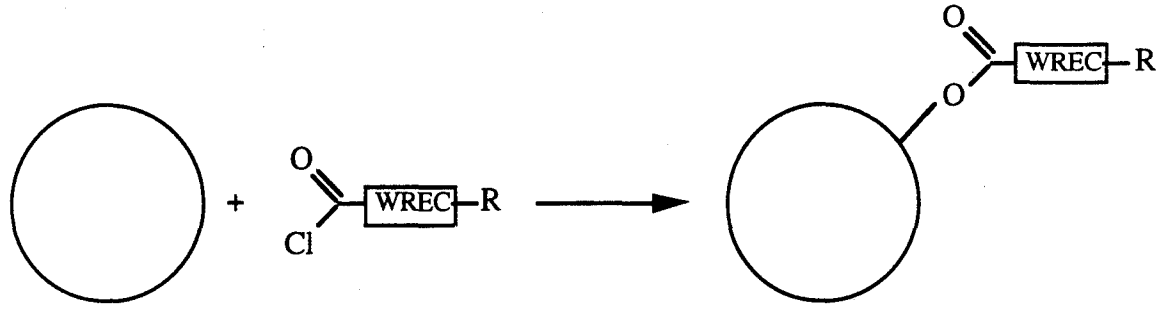

5.2 DYE-MICROSPHERE COUPLING FOR THE DLMS FEASIBILITY STUDY

For the DLMS-based memory system we have labeled the polystyrene microspheres with the dyes, both Nile Red and aminosulfoneazobenzene. In general, the surface of the dye-labeled microsphere was smooth, as expected. But, a few apparent dye residues were also attached to the microsphere surface. The electron micrograph indicating the quality of the dye coupling procedure is shown in Figure 5-1. Successful demonstrations for both non-erasable and erasable DLMS memory systems (discussed in the next Section) indicate that a reasonable coupling between the dyes and the microspheres was achieved.

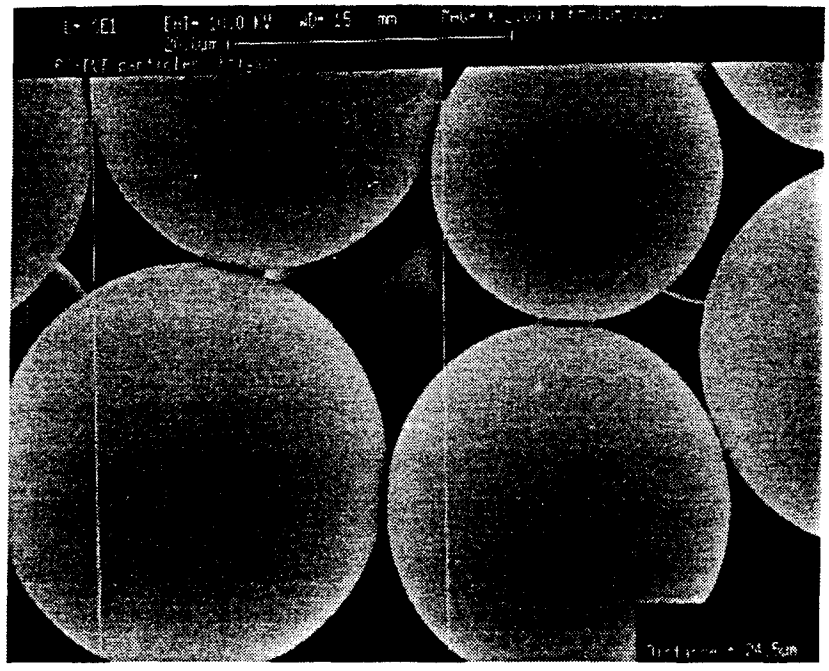

(a)

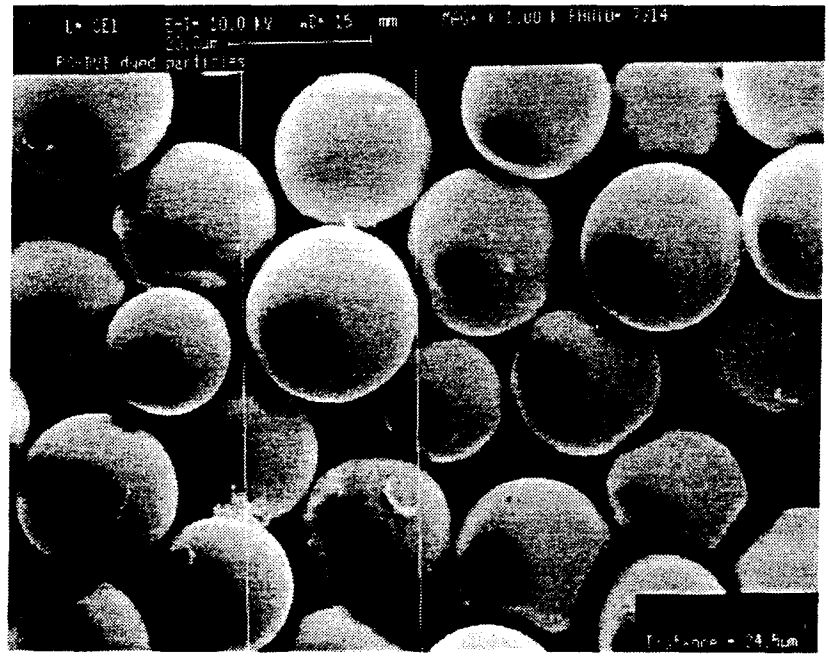

(b)

Figure 5-1. Electron micrographs of 24-μm polystyrene microspheres (a) before and (b) after Nile Red labeling. *A few residuals were found attached to the microsphere surfaces.*

Section 6
FEASIBILITY DEMONSTRATION OF AN ERASABLE DLMS OPTICAL STORAGE SYSTEM

The main goal of this program is to demonstrate the feasibility of the erasable DLMS-based memory system operating at ambient temperature. First, we successfully demonstrated the room temperature W/E/R operations in the frequency domain (in a single spatial pixel). Then, multiple spectral holes were burned (stored) into the sample at ambient temperature. Data retrieval (spectral hole detection) was achieved by scanning the wavelength of the laser probe beam. The erasure was accomplished by a pure optical activation (through UV exposure). Furthermore, we also demonstrated the capability of rewriting information onto the erased sample. In addition, we also conducted an experimental study on the spectral hole-burning process in a non-erasable DLMS-based memory system. We were able to encode nine spectral holes in the frequency domain. To our best knowledge this is the best multiplexing factor that has been reported in the room temperature spectral hole-burning process. The report of this study is included in the Appendix for reference.

6.1 EXPERIMENT FOR ERASABLE ROOM TEMPERATURE PSHB

6.1.1 Sample Preparation

In this study the bi-stable dye was labeled, following the development task for dye/microsphere coupling, on the polystyrene microsphere distribution (in particular, the average diameter of the microsphere distribution ≈24 μm). The dye-labeled microsphere samples were placed on Al-coated slide glasses. [The preparation for the arrangement of dyed microspheres has been described in detail elsewhere (see Appendix)]. The measurement results from three samples (Sample A, Sample B, and Sample C) are reported here. All three samples were prepared from the same batch of the dyed-microsphere distribution (using aminosulfoneazobenzene bi-stable dye).

6.1.2 Experimental Arrangement

The schematic of the experimental setup for room temperature multiple spectral hole burning is depicted in Figure 6-1. Using this set-up, the spectral hole burning and probing were performed with a computer-controlled tunable dye laser pumped by an Ar^+-ion laser. The wavelength of the tunable laser was controlled and scanned with a Coherent Wavescan System. The linewidth of the given laser was estimated to be on the order of 40 GHz. In this experimental arrangement the laser source was split into two arms: a high power beam for hole burning and a weak beam for hole probing. Both beams were recombined and overlapped on the same spatial spot at the sample. A

single lens was then used to condense both beams to approximately 1-mm in diameter at the sample. For reference purposes, the hole burning power was adjusted to ≈500 mW at the initial wavelength of the wavelength scanning range. The peak power of the probe beam was set ≈50 μW at the same reference point.

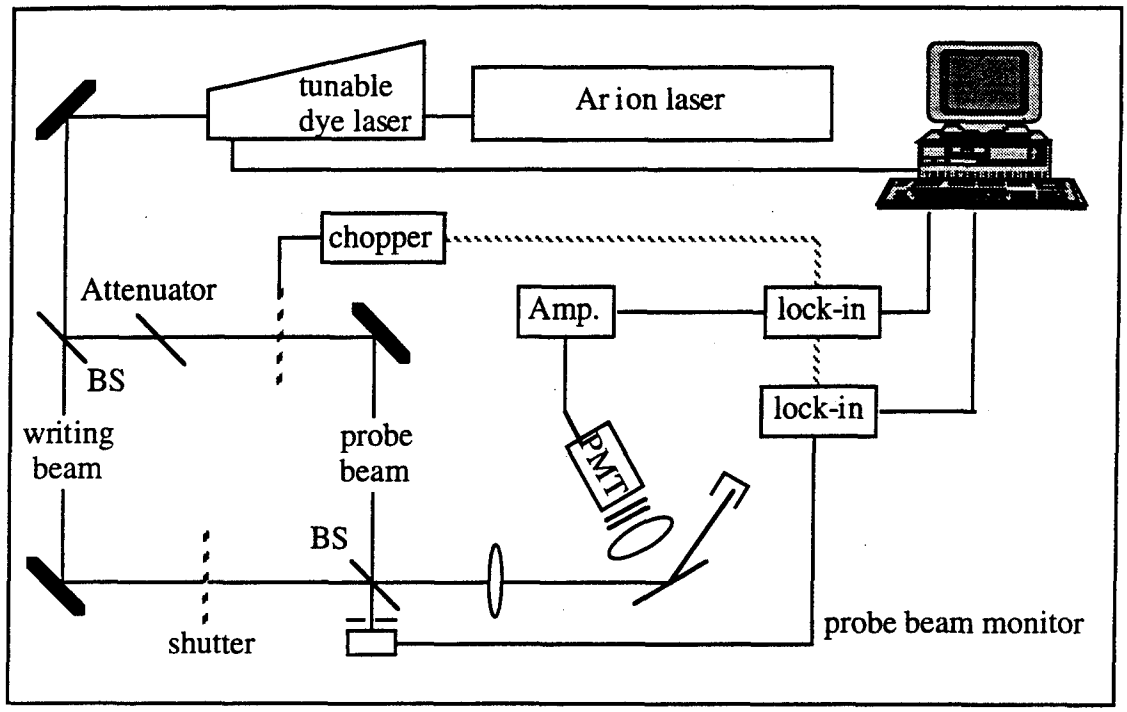

Figure 6-1. Experimental setup for evaluating room-temperature erasable DLMS-based memory operations

The excited fluorescence from the sample was collected through a single lens and detected by a Photomultiplier Tube (PMT). While both hole burning and probing beams were incident at the sample plane at ≈60°, the PMT was positioned at a normal to the sample substrate. To improve the signal-to-noise ratio, a chopper was employed in the arm of the probe beam. To balance the laser intensity fluctuations, the probe beam intensity was simultaneously monitored so the collected fluorescence signal might be normalized to the probe beam power. Both the fluorescence signal and the probe beam intensity were recorded as functions of the scanning wavelength. The detailed information of the setup is described in the Appendix (with the exception that, here, an additional color filter was added to the PMT to ensure complete suppression of the scattered laser beam).

6.1.3 W/E/R Operations

In this procedure, the spectral holes were burned into the microsphere distribution by directing the burning beam (at a given wavelength) to the sample and they were also probed, through

fluorescence excitation, by scanning the wavelength of the probe beam over the range of interest. A fluorescence excitation spectra was always scanned before any spectral hole was burned into the sample. This initial excitation profile served as a baseline for detecting subsequent spectral holes burned at the same sample spot. As expected, this fluorescence excitation from the dye-labeled microsphere distribution was featureless and approached the spectra from the bulk dye solution. The tunable laser was then tuned to a fixed wavelength for spectral hole burning. The optical erasure was accomplished by exposing the sample to an UV light source. Again, the effect of the optical erasure was verified by the procedure of spectral hole detection.

6.2 RESULTS AND DISCUSSIONS

6.2.1 Spectral Hole Formation

In general, the fluorescence excitation spectrum after the first spectral hole exhibited fairly good hole quality. While the fluorescence excitation signal dramatically decreased after the hole-burning process, the spectral hole was clearly observable (as shown in Figure 6-2 and Figure 6-3). The full width at half maximum (FWHM) of spectral hole was estimated to be less than 1 nm. No "anti-hole" (a relatively increased fluorescence around the burned spectral hole) was observed in any of the samples.

After the first spectral hole formation, additional spectral hole-burnings were attempted. In general, the depths of the previously burned holes decreased as subsequent spectral holes were formed. In Sample A the first hole nearly disappeared (shown in Figure 6-2) as a close laser dose was delivered to burn the second spectral hole. An additional hole-burning (at the same burning wavelength) was required to make the first spectral hole visible. However, it was possible to form multiple spectral holes the first time by following a scheduled hole-burning procedure. This may be accomplished by properly adjusting the laser dose to the formation of each individual spectral hole. For example, in Sample B we burned two spectral holes into the sample under the condition that the hole-burning time for the first spectral hole was twice that for the second spectral hole. As a result, both spectral holes were roughly equal in quality (see Figure 6-3). A similar result was also observed in Sample C.

Finally, a measurement on the ratio of spectral hole depth to the background fluorescence was attempted. In this experiment we were able to sequentially burn three spectral holes into Sample C. Each hole was burned step by step by slowly increasing the laser dose (or exposure time). After each short period of hole-burning, the hole detection procedure was repeated to evaluate the depth/background ratio. The results are revealed in Figure 6-4. While the depth/background of a new spectral hole gradually increased as the corresponding laser dose increased, the depth/background ratios of previously burned holes decreased. Moreover, the growing rate of the newly formed spectral hole decreased as the total laser dose delivered to the sample increased.

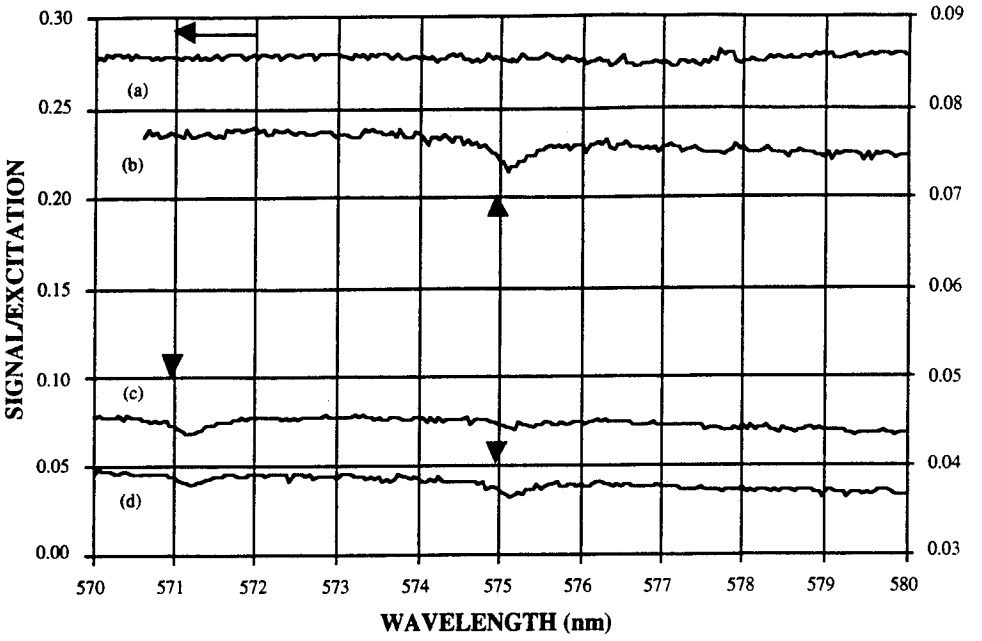

Figure 6-2. Spectral hole formation in Sample A. *Two spectral holes were burned into the sample: curve (a) is the spectrum taken from the fresh sample before the spectral holes were burned, curve (b) shows the first spectral hole after a one-minute hole-burning at 575 nm, curve (c) shows the second spectral hole after the a one-minute hole-burning at 571 nm (note the first hole has nearly disappeared), and curve (d) is the spectrum taken after an additional half-minute hole-burning at 575 nm.*

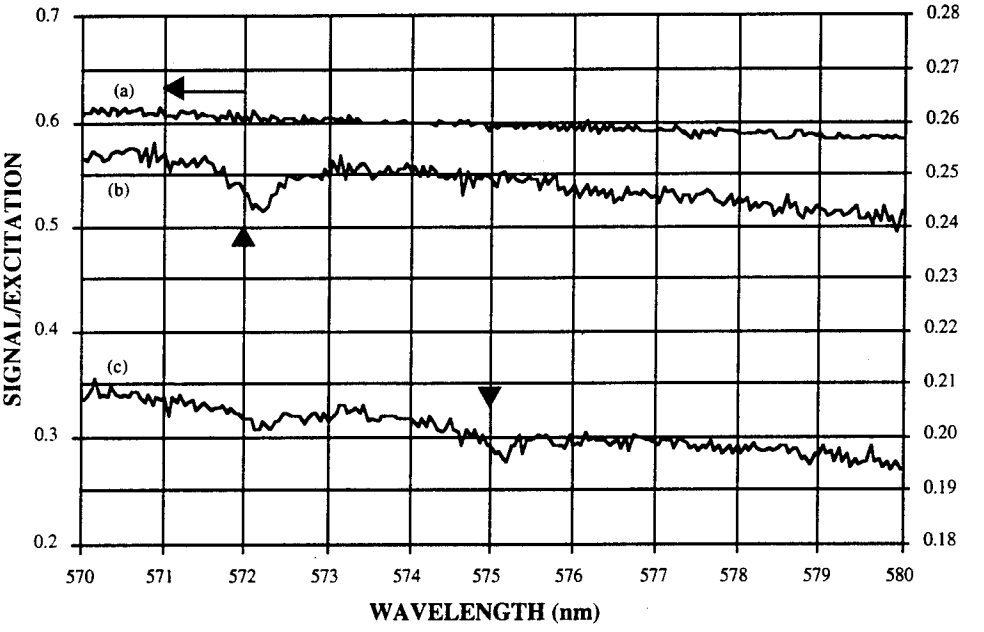

Figure 6-3. Spectral hole formation in Sample B. *Two spectral holes were burned into the sample: curve (a) is the spectrum taken from the fresh sample before the spectral holes were burned, curve (b) shows the first spectral hole after a two-minute hole-burning at 572 nm, curve (c) shows the second spectral hole after a one-minute hole-burning at 575 nm (note both holes are recognizable).*

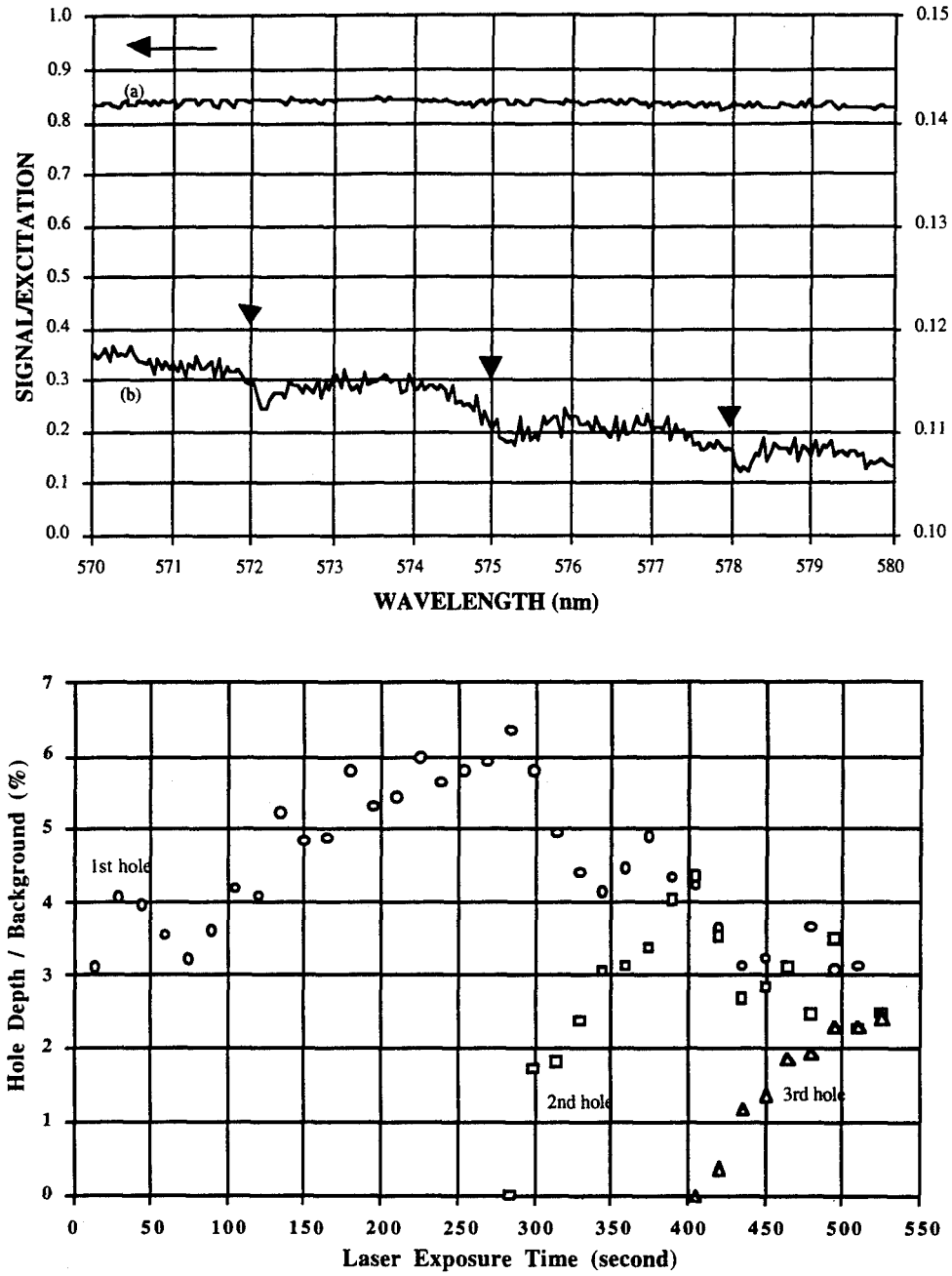

Figure 6-4. Time-resolved measurement on the spectral hole formation in Sample C. *Three spectral holes were successfully burned into the sample (as shown in the upper figure). The ratio of hole depth to the background was plotted as a function of the accumulated hole-burning time.*

6.2.2 Persistence of Spectral Holes

One of the important factors to be considered for all data storage mechanisms is the lifetime of the stored data. To evaluate the persistence of the burned spectral holes, we first kept the samples

in the dark for a period of time after the spectral holes were burned. Then the spectral hole detection procedure was repeated on the same sample. The observations for both Sample A and Sample B were shown in Figure 6-5. They showed that the burned spectral holes retained the original hole quality, although the background fluorescence signal generally increased. In a parallel test a single spectral hole was still clearly observable one hour after the hole was formed (data not shown). Since the stability of spectral holes is expected to be determined by the nature of the bi-stable dyes and the dye/microsphere coupling, the results indicate that to improve the hole persistence further, research should be conducted in both areas.

6.2.3 Spectral Hole Erasure

Optical erasure capability is essential to the optical data storage devices. For the DLMS-based memory system the erasure can be accomplished by exposing the sample to an UV light source. The UV radiation will activate the returning of the photoproducts to the initial configuration. Thus, after the spectral holes were burned into the samples we attempted the optical erasure process. A ten-minute UV exposure was adequate for Sample A to refill two previously burned spectral holes, as illustrated in Figure 6-6. A similar result was also observed in Sample B, where the sample was illuminated for 20 minutes by the same UV light source. There was no erasure selectivity to any individual spectral hole; all spectral holes were simultaneously refilled by the erasure process. On Sample A the erasure was conducted by placing the UV light source directly above the sample (≈1-inch away). For Sample B, a collimator lens was inserted between the light source and the sample to ensure the sample would not receive heat radiated from the light source. No significant difference was observed for either one.

6.2.4 Spectral Hole Rewriting

In order to ensure the chemical configuration has been properly restored, rather than being converted to some completely different structures, we went a step further to repeat the spectral hole-burning in a freshly erased sample. Afterwards, a new spectral hole (at a different hole-burning wavelength) was then burned into Sample B. The newly formed spectral hole exhibited a similar hole quality (with reduction in fluorescence signal), as is clearly shown in Figure 6-7. Again, this particular spectral hole could be re-erased by the same UV erasure procedure. The evidence of erasure is shown in Figure 6-8.

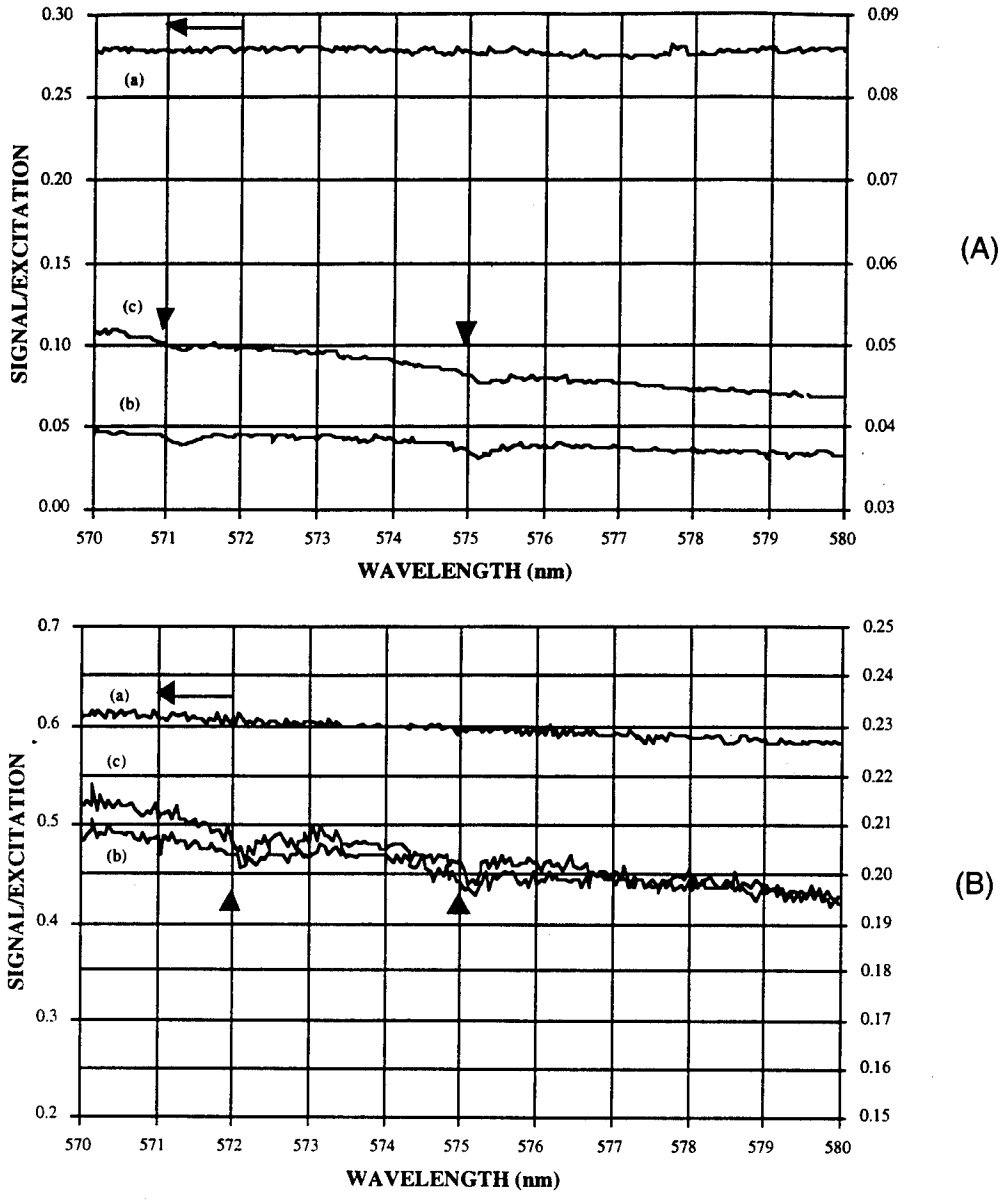

Figure 6-5. Persistence evaluation of the burned spectral holes. *After two spectral holes were burned, the samples were kept in the dark for 20 minutes and the spectral holes were re-probed on two samples: Sample A [see (A) above] and Sample B [see (B)]. Here curve (b) is the spectrum right after the hole-formation and curve (c) is the re-probed spectrum.*

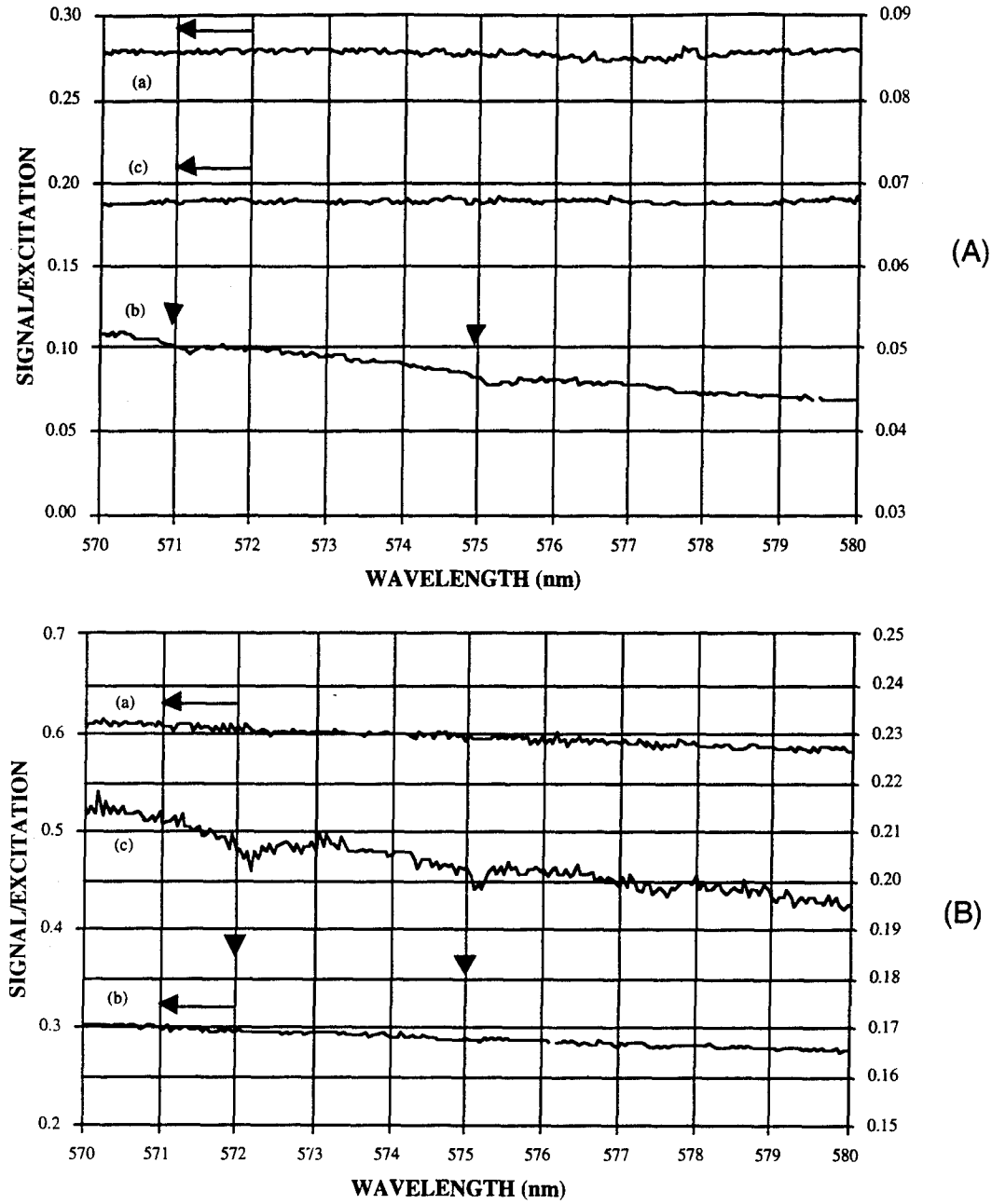

Figure 6-6. Optical erasure of the burned spectral holes. *After two spectral holes were burned into the samples, optical erasure was attempted on two samples. Sample A [see (A) above] was submitted to 10 minutes' exposure; Sample B [see (B)], to 20. Here curve (b) is the spectrum right after the holes formation and being kept in the dark for 20 minutes, and curve (c) is the spectrum measured after the UV erasure.*

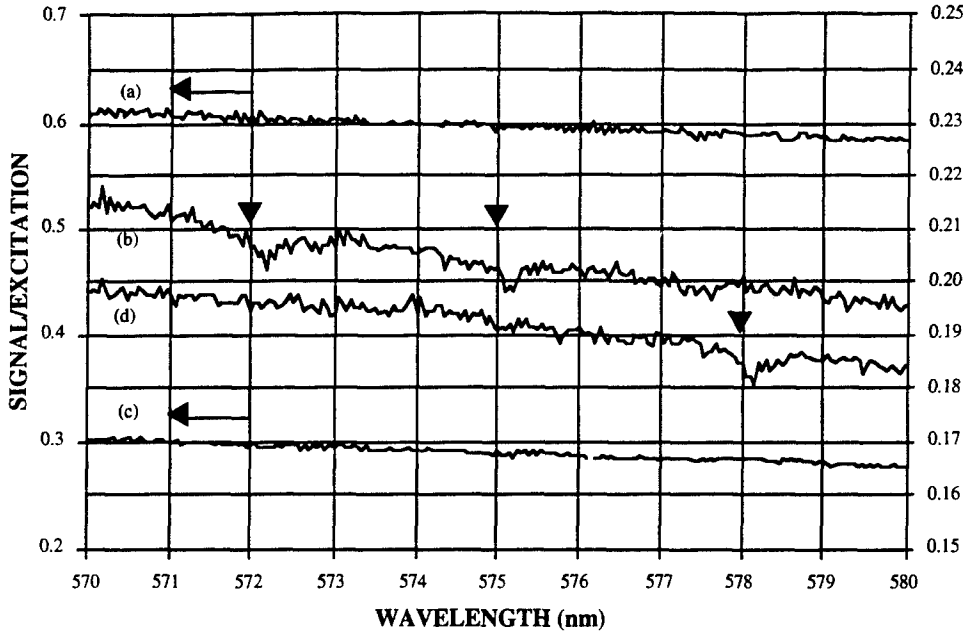

Figure 6-7. Rewriting of spectral hole in a freshly-erased sample (Sample B). *Two spectral holes were burned into the sample: curve (a) is the spectrum taken from the fresh sample before the spectral holes were burned, curve (b) shows the two previously burned spectral holes, curve (c) shows the spectrum after the optical erasure, and curve (d) shows the newly formed spectral hole after a one-minute hole-burning at 578 nm.*

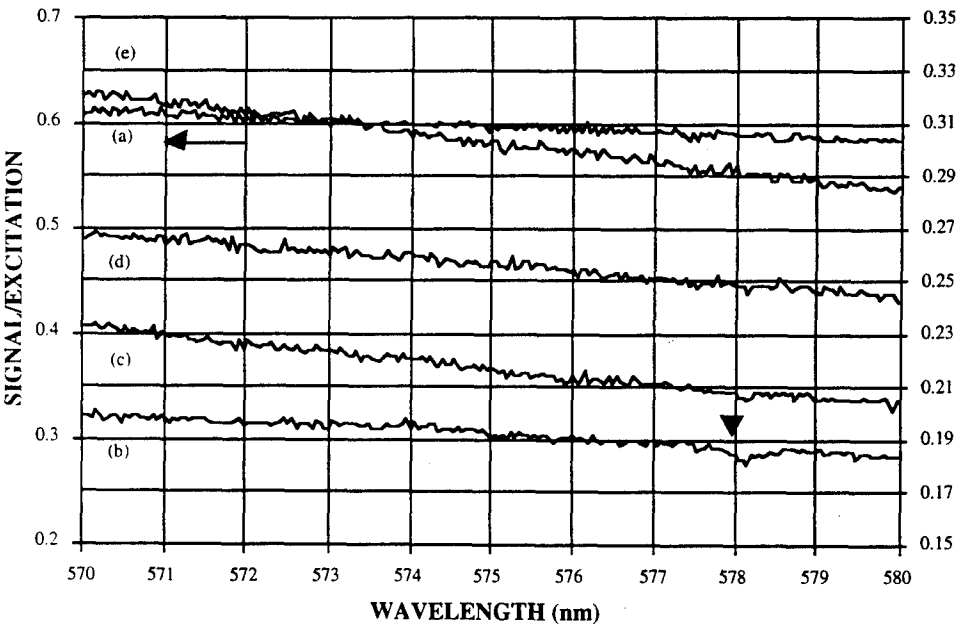

Figure 6-8. Optical erasure conducted on Sample B after the procedure described in Figure 6-7. *Here, curve (a) is the spectrum taken from the fresh sample before the spectral holes were burned, curve (b) is the newly formed spectral hole described in the previous figure. Curve (c) showed the spectrum after one-minute of UV erasure. Curve (d) and curve (e) are the spectra measured after five- and sixty-minute UV erasures, respectively.*

Section 7
REFERENCES

1. U. P. Wild and A. Renn, J. Mole. Electr. **7,** 1 (1991).
2. P.B. Derra, A. Ghafoor, M. Guizani, S.J. Marcinkowski, and P.A. Mitkas, Proc. IEEE **72,** 1797 (1989).
3. S. Esener in SPIE Critical Reviews Series, Vol. **1150**, pp. 113-119 (1990).
4. K. Ishii, T. Takeda, K. Itao, and R. Kaneko, SPIE Vol. **1248**, pp. 2-9 (1990).
5. H. Suzuhi, Nonlinear Opt. **1**, 333 (1991).
6. L. d'Auria, J. P. Huignard, C. Slezak, andE. Spitz, Appl. Opt. **13**, 808 (1974).
7. F. H. Mok, Opt. Lett. **18**, 915 (1993).
8. S. Hunter, F. Kiamilev, S. Esener, D. A. Parthenopoulos, and P. M. Rentzepis, Appl. Opt. **29**, 2058 (1991).
9. G. Castro, D. Haarer, R.M. Macfarlane and H.P. Trommsdorff, U.S. Patent, No. 4,101,976 (1978),
10. W.E. Moerner, ed., "Persistent Spectral Hole Burning Science and Applications," (Spring-Verlag, New York, 1988).
11. A. Renn and U. P. Wild, Appl. Opt. **26**, 4040 (1987).
12. C. De Caro, A. Renn and U.P. Wild, Appl. Opt. **30**, 2890 (1991).
13. A. Kurita, T. Kushida, T. Izumitani, and M. Matsukawa, Opt. Lett. **19,** 314 (1994).
14. R. Ao, S. Jahn, L. Kummeri, R. Weiner and D. Haarer, Jpn. J. Appl. Phys. **31,** 693 (1992).
15. R. Menzel and P. Witte, J. Chem. Phys. **87,** 6769 (1987).
16. R. Jaaniso and H. Bill, Europhys. Lett. **16,** 569 (1991).
17. J. Zhang, S. Huang, and J. Yu, Opt. Lett. **17**, 1146 (1992).
18. K. Holloday, C. Wei, M. Croci, and U.P. Wild, J. Limin. **53**, 227 (1992).
19. K. Hirao, S. Todaroki, D.H. Cho, and N. Soga, Opt. Lett. **18,** 1586 (1993).
20. K. Hirao, S. Todoroki, and N. Soga, J. Lumin. **55,** 217 (1993).
21. K. Hirao, S. Todorki, K. Tanaka, N. Saga, T. Izumitani, A. Kurita, and T. Kushida, J. Non-Cryst. Solids, 152, 267 (1993).
22. S. Arnold and C.T. Liu, Opt. Lett. **16,** 420 (1991).
23. K. Kang, A.D. Kepner, Y.Z. Hu, S.W. Koch, N. Peyghambarian, C.-Y. Li, T. Takada, Y. Kao, and D. Mackenzie, Appl. Phys. Lett. **64,** 1487 (1994).
24. P.W. Barber and R. K. Chang, eds., "Optical Effects Associated with Small Particles," (World Science, New Jersey, 1988).

25. B. Kohler, S. Bernet, A. renn, and U. P. Wild Opt. Lett. **18,** 2144 (1993).
26. M. Mitsunaga, N. Uesugi, H. Sasaki, and K. Karaki, Opt. Lett. **19,** 752 (1994).
27. S. Arnold, J. Comunale, W.B. Whitten, J.M. Ramsey, and K.A. Fuller, JOSA. B **9,** 819 (1992).
28. C. Xu et al., Macromolecules, 26, 5303 (1993).
29. C. Xu et al., Chemistry of Materials, 5,1439 (1993).
30. D. Zou et al., J. Polym. Sci., Part A: Polym. Chem., 28,1909 (1990).
31. K. Gandhi, et al., J. Polym. Sci., Part B: Polym. Phys., 28, 2707 (1990).
32. M . Park, et al ., Polym . Eng . and Sci ., 30,1158 (1990) .
33. Z. Y. Ding, et al., J. Polym. Sci., Part B: Polym. Phys., 29,1035 (1991).
34. D. Zou et al., J. Polym. Sci., Part A: Polym. Chem., 30,1463 (1992).
35. L. Sun et al., Polym. Eng. and Sci., 32,1418 (1992).
36. Z. Y. Deng, et al., J. Polym. Sci., Part B: Polym. Phys., 30,1189 (1992).
37. L. Sun, et al., Polym. Eng. and Sci., 32, 777 (1992).
38. D. Zou, et al., J. Polym. Sci., Part A: Polym. Chem., 30, 137 (1992).
39. D. Zou, et al., J. Polym. Sci., Part A: Polym. Chem., 30, 2443 (1992).
40. L. Sun et al., Polym. Eng. and Sci., 33,1308 (1993).
41. G.K. S. Prakash et. al., SYLLETT, 1, 39 (1991).
42. G.A. Olah, et al., J. Org. Chem., 58, 6900 (1993).

APPENDIX

DEMONSTRATION OF ROOM-TEMPERATURE, MULTIPLE SPECTRAL HOLE BURNING IN A SUBMICRON-SIZED MICROSPHERE DISTRIBUTION

C.-S. Wu, A. Au, and U. Efron

Hughes Research Laboratories, 3011 Malibu Canyon Road, Malibu, CA 90265

Q.-S. Li and L.R. Dalton

Chemical Engineering Department and Chemistry Department, University of Southern California, Los Angeles, California, 90089

ABSTRACT

Morphology-dependent resonances in microspheres provide a fundamental basis for wavelength coding. Recently, we have investigated multiple spectral hole-burning in a dye-labeled submicron microsphere distribution with the potential of frequency-domain data storage at room temperature. We report here results which demonstrate the capability of encoding multiple spectral information on such a submicron microsphere distribution.

Persistent spectral hole burning (PSHB) has long attracted considerable attention for its potential application in extremely-multiplexed frequency-domain optical data storage.[1] The key feature is that multiple 2-D data pages may be encoded in spectral frequency and stored in a single spatial space. Remarkable progress has been reported in PSHB material study[2-4] and technology development,[5] where the basic spectral hole formation is limited by the need for cryogenic operation. At the same time, room-temperature PSHB is emerging as a possibility for frequency-domain data storage, even though the room-temperature operation may reduce the multiplexing factor in the frequency domain.[6] Thus, room-temperature PSHB has attracted increased attention in research efforts on both materials and device configurations. For example, intensive studies have been devoted to the development of room-temperature PSHB materials such as organic solutions,[7] Sm^{2+}-doped crystals,[8-10] and Sm^{2+}-doped glasses.[11-14] In this research, two to three spectral holes were successfully burned into the samples and retrieved at room temperature. In addition, a new room-temperature PSHB mechanism has been proposed and it was observed in dye-labeled microparticles.[15] Room temperature spectral hole-burning was also reported in sol-gel CdS quantum dots at room temperature.[16]

Relying on narrow electromagnetic morphology dependent resonances (MDR's) as wavelength selection tools, digital information can be frequency-encoded into a distribution of dye-labeled microspheres. The advantage of such MDR-based spectral hole burning memory functions lies in their capability of room-temperature operation. One spectral hole was first demonstrated in a large-size polystyrene microsphere distribution (average diameter $\langle d \rangle \approx 24$ μm).[15] It was later reported that a few (number unspecified) spectral holes were burned into the same sample.[17] This demonstration immediately raised a concern (based on the assumption that the large size microspheres were essential) that the ultimate data storage density might be severely degraded.[17] It also promoted research interest as to whether the same room-temperature spectral hole-burning process could be observed in a smaller-size microsphere distribution. Realizing the importance of wavelength-multiplexing capability in frequency-domain optical data storage, we have recently studied room-temperature multiple spectral hole-burning in a dye-labeled submicron microsphere distribution. In this Letter we present experimental results demonstrating the capability of encoding multiple spectral information on a submicron-sized microsphere distribution.

For experimental convenience, the photolyzing medium (Nile Red) and dye-labeling procedure were adapted following Arnold's published paper.[15] Here the dye was labeled on a submicron-sized polystyrene microsphere distribution (average diameter of ≈0.783 μm). To improve their size uniformity, the submicron polymer microspheres were fabricated by a semi-continuous emulsion polymerization method.[18,19] In this experiment the dye-labeled microsphere samples were placed on Al-coated slide glasses. While microspheres which are loosely connected laterally have little effect on the MDR conditions of each corresponding microsphere,[20] optical coupling

between stacked microspheres can make a significant contribution to the MDR conditions of the involved microspheres.[21] To suppress coupling between stacked microspheres, careful attempts were made to compactly pack the dye-labeled microspheres in one single layer.

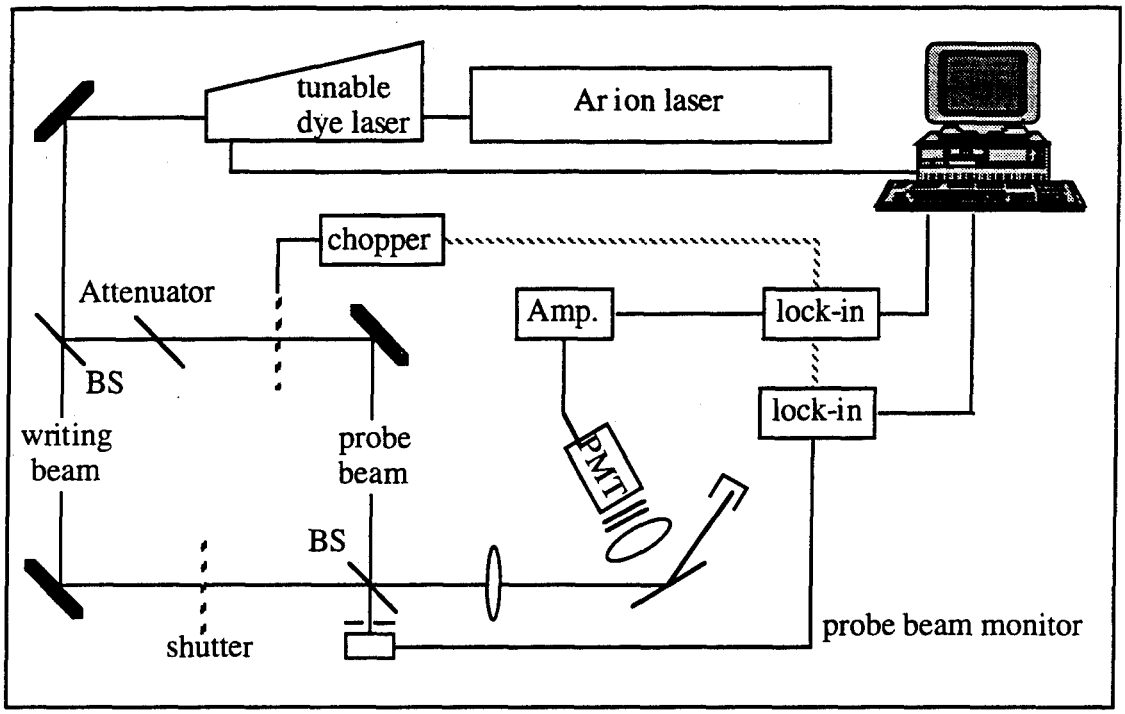

Figure 1. Experimental setup for room-temperature spectral hole burning in submicron-sized microspheres. *A computer-controlled tunable dye laser is used for wavelength selection. During spectral hole-burning, the writing beam is unblocked and the laser beam is condensed to ≈ 1mm at the sample. The spectral hole is detected through fluorescence excitation, while the writing beam is blocked. For this experiment both the fluorescence signal and the probe beam power were monitored and processed by lock-in amplifiers. The data were simultaneously fed into a computer data-acquisition system: in this way the fluroescence signal could be normalized to the probe beam intensity to reduce the effect of laser fluctuations.*

The schematic of the experimental setup for room-temperature multiple spectral hole-burning is depicted in Figure 1. In this set-up, the spectral hole burning and probing were performed with a computer-controlled tunable dye laser (Coherent Model 699 with a standing wave cavity) pumped by an Ar^+-ion laser. The tunable laser was operated with Pyrromethane 556 (Exciton), and its wavelength was controlled and scanned with a Coherent Wavescan System. The linewidth of the given laser was estimated to be on the order of 40 GHz. In this experimental arrangement, the laser source was split into two arms: a high power beam for hole-burning and a weak beam for hole probing. Both beams were recombined and overlapped on the same spatial spot at the sample. A single lens was then used to condense both beams to approximately 1-mm in diameter at the sample. For reference purposes, the hole-burning power was adjusted to ≈400 mW at the initial

wavelength of the wavelength scanning range. The peak power of the probe beam was set ≈4 μW at the same reference point.

In this procedure, the spectral holes were burned into the microsphere distribution by directing the burning beam (at a given wavelength) to the sample and probed, through fluorescence excitation, by scanning the wavelength of the probe beam over the range of interest. The excited fluorescence was collected through a single lens and detected by a Photomultiplier Tube (PMT). While both hole-burning and probing beams were incident at the sample plane at ≈60°, the PMT was positioned at a normal to the sample substrate. Two sharp color filters (03-FCG-098 and 03-FCG-101 from Melles Griot) were further added in front of the PMT to completely suppress the residual laser scattering. To improve the signal-to-noise ratio, a chopper (Princeton Applied Research) was employed in the arm of the probe beam. The chopping frequency was set at 500 Hz. The fluorescence signal was then amplified by an amplifier (Keithley 427) and processed by a lock-in amplifier (Princeton Applied Research 5204). To balance the laser intensity fluctuations, the probe beam intensity was simultaneously monitored so the collected fluorescence signal might be normalized to the probe beam power. The probe beam intensity was then monitored by an additional lock-in amplifier (Ortec Brookdeal 9503-SC). Both the fluorescence signal and the probe beam intensity were recorded as functions of the scanning wavelength. To minimize destructive readout effect, the spectral hole detection was typically scanned within 300 s; for each scan the accumulated laser dose at the sample was kept much lower than the dose for the spectral hole formation.

In our experiment, a fluorescence excitation spectra was first scanned before any spectral hole was burned in the sample. This initial excitation profile served as a baseline for detecting subsequent spectral holes burned at the same sample spot. As expected, this fluorescence excitation from the dye-labeled microsphere distribution was featureless and approached the spectra from the bulk dye solution. The tunable laser was then tuned to a fixed wavelength for spectral hole burning. Figure 2(a) shows the fluorescence excitation spectra after the first spectral hole burning; the fluorescence signal was normalized to the probe beam intensity. While the fluorescence excitation dramatically decreased after the first hole burning, the spectral hole was clearly observable. The full width at half maximum (FWHM) of the spectral hole was ≈1 nm and its depth was on the order of 12% of the background. The result was similar to what was observed in the large-size microsphere distribution.[15]

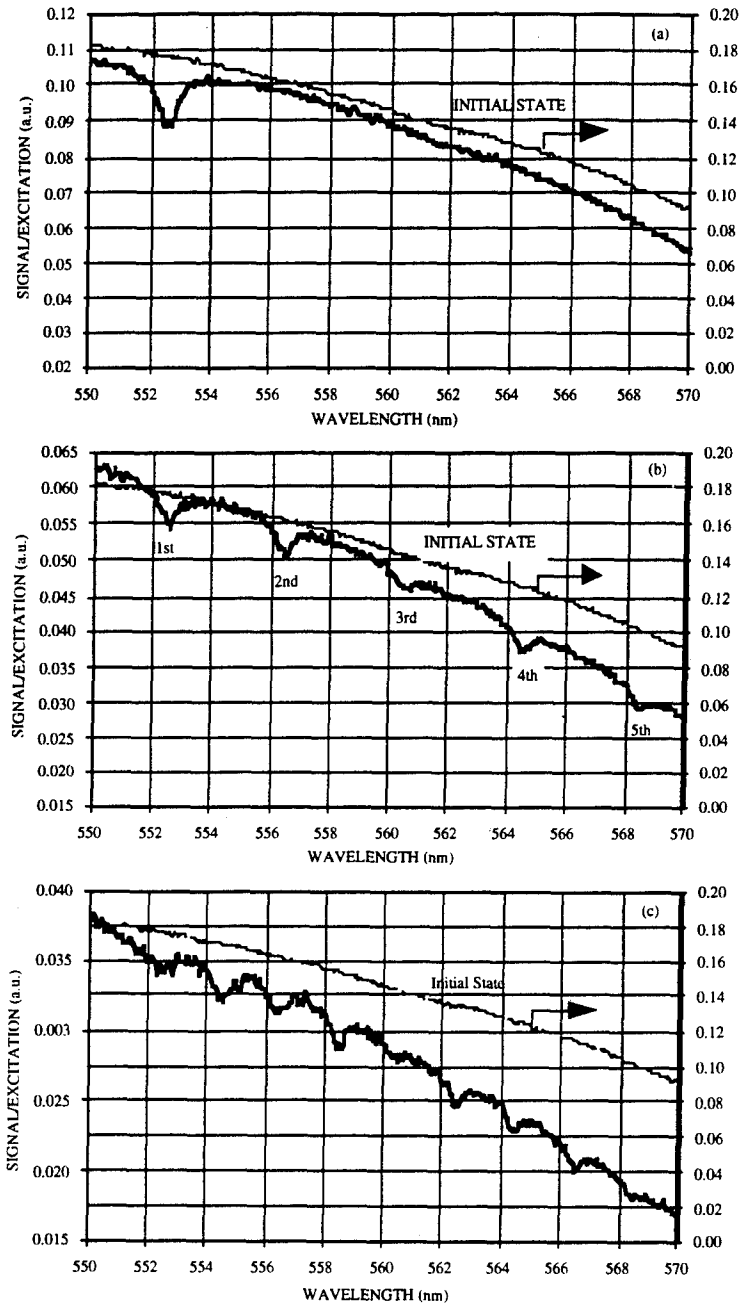

Figure 2. Fluorescence excitation for spectral hole-burning in Nile Red-coated submicron-sized polystyrene microspheres. *(a) After the first spectral hole was burned in the sample. (b) After four more spectral holes were burned at the same sample spot. One of the spectral holes was burned for a reduced hole formation period. After each spectral hole burning the fluorescence excitation was scanned to reveal the existence of the spectral holes. (c) After four more spectral holes were burned into the same sample spot. No intermediate fluroescence excitation scanning was conducted between the hole burnings.*

Four more spectral holes were then sequentially burned into the same sample spot. After each hole burning, the fluorescence excitation was scanned through the whole spectrum range. The depths of the previously burned holes decreased as subsequent spectral hole formations were burned into the sample. In addition, the third spectral hole was burned for only one minute instead of the two-minute burning administered for the rest of the spectral holes. As noted in Figure 2(b), the depth of this particular hole was shallower than the depths of the others, while the width of the spectral hole was roughly the same. This suggests that, under the given experimental conditions, the saturation effect did not play a significant role in determining the widths of the spectral holes.

Afterward, four more spectral holes were burned into the same sample spot without interruption and a fluorescence excitation was conducted only after all nine spectral holes had been burned. The final fluorescence excitation spectra is shown in Figure 2(c). All nine spectral holes exhibited a substantial hole depth relative to the background and the spectral holes can be clearly recognized. In particular, note that the final hole probing was conducted ≈1.5 hours after the first spectral hole was burned. As is shown in Figure 3, the existence of multiple holes was most pronounced when the data were further normalized to the baseline before hole-burning. What is of particular interest is that although the ratio of spectral hole depth to the fluorescence background may be decreased by the subsequent hole-burning, the ratio tends to be saturated to a constant level for all spectral holes (except the third spectral hole).

Furthermore, we observed a consistent spectral shift (a noticeable red shift, ~0.5 nm) in all nine burned spectral holes when comparing the central wavelength of the burned spectral holes with the wavelength of the corresponding burning beam. All spectral holes exhibited a common "red shift" to the corresponding burning wavelength. Attempting a replication, we repeated the hole burning process (up to three spectral holes) in a distribution of 24-μm Nile Red-coated microspheres, and no significant spectral shift was observed. While it is consistent with the single hole-burning result reported in Ref.[15], it is definitely not so for the same sample measured on a polished aluminum surface.[20] It is currently not clear what os the mechanism responsible for the observed spectral shifts. The spectral shifts may be attributable to a dynamic shifting of MDR conditions which may occur when the dye molecules attached to the microspheres are bleached by the writing beam and undergo a change in the physical properties. The shift of the MDR conditions can then alter the resonance size of the microspheres during the hole-burning. As a result, a spectral shift may be expected when the hole is probed after the hole formation. In this case the spectral shift could be expected to be more pronounced for small microsphere sizes.

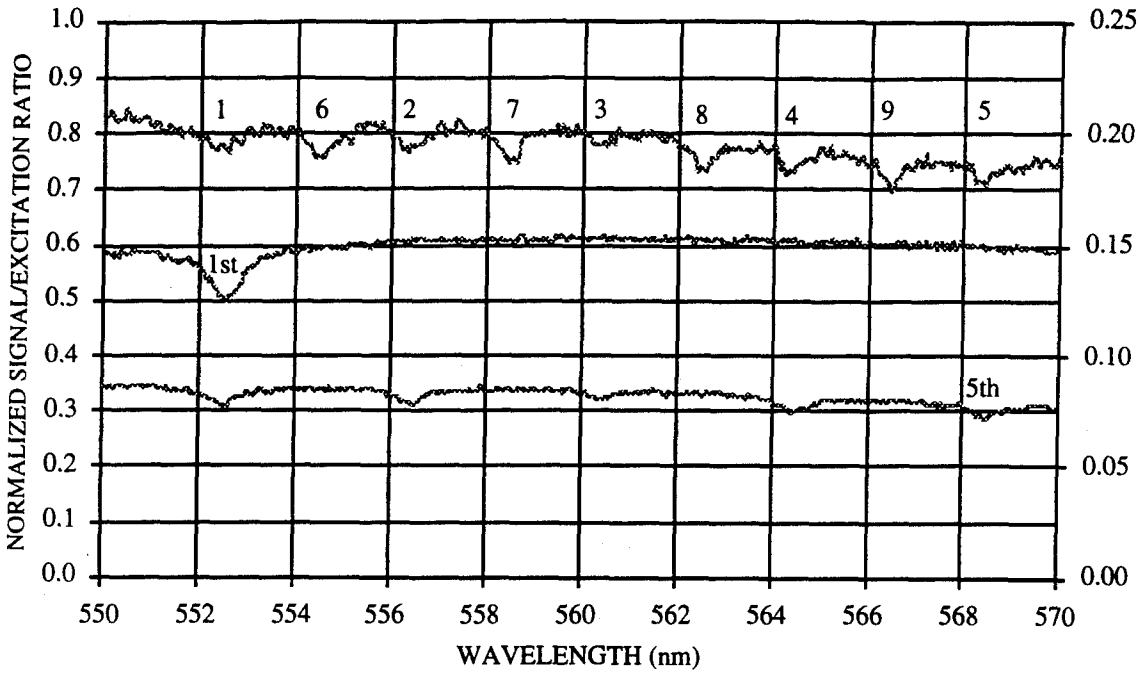

Figure 3. Normalized fluorescence excitation for spectral hole burning in the same sample as shown in Figure 2. *The fluorescence excitation signal was further normalized to the baseline measurement (fresh sample before spectral hole-burning). The process removes the wavelength-dependence of fluorescence quantum efficiency and the detectors.*

In conclusion, we have demonstrated spectral hole-burning on a submicron-sized microsphere distribution. The wide fluorescence excitation band of the dye supports a fairly large wavelength multiplexing factor to encode and retrieve data, at room temperature. In addition, we have also observed a consistent spectral shift between the burning wavelength and the central wavelength of the formed spectral hole. In addition, despite the large reduction in the sizes of the microsphere, the quality of spectral holes burned in the submicron-sized microsphere distribution is comparable to that reported in a 24-μm microsphere distribution. Since the hole width reflects the Q factor of the MDR's in the dye-labeled microspheres, non-radiative losses—such as dye absorption and surface scattering—may play an important role in the spectral hole quality.[22-24] In the future, the effect of the dye-labeling process on the quality of spectral hole-burning, especially on the capability of multiple spectral hole-burning, will be studied.

We gratefully acknowledge the support of U.S. Air Force Rome Laboratory contract F30602-93-C-0158. The authors would also like to thank Dr. C.J. Gaeta of Hughes Research Laboratories for valuable technical assistance.

REFERENCES

1. W. E. Moerner, ed., "Persistent Spectral Hole-Burning: Science and Applications," Springer, Berlin (1988).

2. H. Suzuki and T. Shimada, "Subnanosecond burning of persistemt spectral holes by donor-acceptor electron transfer in tetraphenylporphine/p-benzoquinone systems," Appl. Phys. Lett. **59,** 1814 (1991).

3. R. Yano, M. Mitsunaga, and N. Uesugi, "Ultralong optical dephasing time in $Eu^{+3}:Y_2SiO_5$," Opt. Lett. **16,** 1884 (1991).

4. T. Tani and Y. Sakakibara, "Design of photochemical hole burning materials: Burning process in hydrogen bonding and proton transfer molecular system," Jpn. J. Appl. Phys. **31,** 783 (1992).

5. M. Mitsunaga, N. Uesugi, H. Sasaki, and K. Karaki, "Holographic motion picture by $Eu^{3+}:Y_2SiO_5$," Opt. Lett. **19,** 752 (1994).

6. R. Ao, S. Jahn, L. Kummeri, R. Weiner and D. Haarer, "Spatial resolution and data addressing of frequency doamin optical storage materials in the near IR regime," Jpn. J. Appl. Phys. **31,** 693 (1992).

7. R. Menzel and P. Witte, "Observation of photophysical hole burning on solutions of triphenylmethane dyes at room temperature with ns laser pulse," J. Chem. Phys. **87,** 6769 (1987).

8. R. Jaaniso and H. Bill, "Room temperature persistent spectral hole burning in Sm-doped $SrFCl_{1/2}Br_{1/2}$ mixed crystals," Europhys. Lett. **16,** 569 (1991).

9. J. Zhang, S. Huang, and J. Yu, "High-temperature stability of a spectral hole burnt in Sm-doped SrFCl crystals," Opt. Lett. **17**, 1146 (1992).

10. K. Holloday, C. Wei, M. Croci, and U. P. Wild, "Spectral hole-burning measurements of optical dephasing between 2-300 K in Sm^{2+} doped substitutionally disordered microcrystals," J. Limin. **53**, 227 (1992).

11. K. Hirao, S. Todaroki, D. H. Cho, and N. Soga, "Room-temperature persistent hole burning of Sm^{2+} in oxide glasses," Opt. Lett. **18,** 1586 (1993).

12. K. Hirao, S. Todoroki, and N. Soga, "Room temperature persistent spectral hole burning of Sm^{2+} in fluorohafnate glasses," J. Lumin. **55,** 217 (1993).

13. K. Hirao, S. Todorki, K. Tanaka, N. Saga, T. Izumitani, A. Kurita, and T. Kushida, "High temperature persistent spectral hole burning of Sm^{2+} in fluorohafnate glasses," J. Non-Cryst. Solids, 152, 267 (1993).

14. A. Kurita, T. Kushida, T. Izumitani, and M. Matsukawa, "Room-temperature persistent spectral hole burning in Sm^{2+}-doped fluoride glasses," Opt. Lett. **19,** 314 (1994).

15. S. Arnold and C.T. Liu, "Room-temperature microparticle-based persistent spectral hole burning memory," Opt. Lett. **16,** 420 (1991).

16. K. Kang, A.D. Kepner, Y.Z. Hu, S.W. Koch, N. Peyghambarian, C.-Y. Li, T. Takada, Y. Kao, and D. Mackenzie, "Room temperature spectral hole burning and elimination of photodarkening in sol-gel derived CdS quantum dots," Appl. Phys. Lett. **64,** 1487 (1994).

17. D.H. Freedman, "Drawing a bead on superdense data storage," Research News **March,** 1213 (1992).

18. Z. Y. Ding, J. J. Aklonis, and R. Salovey, "Model filled polymers. VI. Determination of the crosslink density of polymetric beads by swelling," J. Polym. Sci.: Polym. Phys. **29**, 1035 (1991).

19. Z.Y. Ding, S, Ma, D. Kriz, J.J. Aklonis, and R. Salovey, "Model filled polymers. IX. Synthesis of uniformly crosslinked polystyrene microbeads," J. Polym. Sci.: Polym. Phys. **30**, 1189 (1991).

20. S. Arnold, J. Comunale, W.B. Whitten, J.M. Ramsey, and K.A. Fuller, "Room-temperature microparticle-based persistent hole-burning spectroscopy," JOSA. B **9**, 819 (1992).

21. K.A. Fuller, "Optical resonances and two-sphere systems," Appl. Opt. **30**, 4716 (1991).

22. H. S. Bennett and G.J. Rosasco, "Resonances in the efficiency factors for absorption: Mie scattering theory," Appl. Opt. **17**, 491 (1978).

23. P. Chylek, J.T. Kiehl, and M.K.W. Ko, "Narrow resonance structure in the Mie scattering characteristics," Appl. Opt. **17**, 3019 (1978).

24. H.-B. Lin, A.L. Huston, J.D. Eversole, and A.J. Campillo, "Internal scattering effects on microdroplet resonant emission structure," Opt. Lett. **17**, 970 (1992).

*U.S. GOVERNMENT PRINTING OFFICE: 1995-610-126-50178

Rome Laboratory

Customer Satisfaction Survey

RL-TR-_____

Please complete this survey, and mail to RL/IMPS, 26 Electronic Pky, Griffiss AFB NY 13441-4514. Your assessment and feedback regarding this technical report will allow Rome Laboratory to have a vehicle to continuously improve our methods of research, publication, and customer satisfaction. Your assistance is greatly appreciated.
Thank You

_____

_____

Organization Name:_____(Optional)

Organization POC: _____(Optional)

Address:_____

1. On a scale of 1 to 5 how would you rate the technology developed under this research?

5-Extremely Useful 1-Not Useful/Wasteful

Rating_____

Please use the space below to comment on your rating. Please suggest improvements. Use the back of this sheet if necessary.

2. Do any specific areas of the report stand out as exceptional?

Yes___ No_____

If yes, please identify the area(s), and comment on what aspects make them "stand out."

3. Do any specific areas of the report stand out as inferior?

Yes___ No___

If yes, please identify the area(s), and comment on what aspects make them "stand out."

4. Please utilize the space below to comment on any other aspects of the report. Comments on both technical content and reporting format are desired.